Cenozoic compressional tectonics and post-glacial landsliding at Forkastningsfjellet, Spitsbergen, Svalbard

Andreas Albertsen

Thesis submitted for the degree of
Master of science in Geology
60 credits

Department of Geosciences
Faculty of mathematics and natural sciences

UNIVERSITY OF OSLO

Spring 2016

Cenozoic compressional tectonics and post-glacial landsliding at Forkastningsfjellet, Spitsbergen, Svalbard

Andreas Albertsen

Cenozoic compressional tectonics and post-glacial landsliding at Forkastningsfjellet, Spitsbergen, Svalbard

http://www.duo.uio.no/

Printed: Reprosentralen, University of Oslo

Cenozoic compressional tectonics and post-glacial landsliding at Forkastningsfjellet, Spitsbergen, Svalbard

Andreas Albertsen

June 1, 2016

Contents

List of Figures

Preface

Abstract

The area around Forkastningsfjellet, Spitsbergen, considered to contain Cenozoic compressional structures, presumably related to the West Spitsbergen Fold and Thrust Belt (WSFTB), as well as post-glacial landslide structures. Structural geological mapping was done over 3 weeks in July-August 2015, aiming to describe the different styles of deformation present in the study area. Models for both the Cenozoic structures and the post-glacial landslide-related structures are discussed.

The dominant Cenozoic structures are top-to-the-west reverse faults, interpreted as back-thrusts in the context of the WSFTB. The proposed model for these faults have the major fault, Revneset Reverse Fault, as an out-of-sequence thrust relative to the numerous minor faults. The minor reverse faults terminate somewhere above a glacial erosional surface, and several models for their formation are discussed.

The landslide structures include SW-striking fault scarps and NW/SE-striking counterscarps. A retrogressive slumping landslide model is suggested as the mechanism of formation for the landslides. Internal deformation structures within fault blocks show significant variation in deformation style between the different stratigraphical units.

0.1 Acknowledgments

First and foremost, a huge thanks to my supervisors, Professor Emeritus Arild Andresen and Associate Professor Ivar Midtkandal, without whose support and assistance, both in the field and during the writing process, this thesis would not have existed. Thanks to Fridtjof Andersen for support, companionship and fruitful discussion both in the field and in the study hall. To the LoCrA project for financial support, without which the field work for this thesis would not have been possible. To UNIS for invaluable training and logistical support in the field. To Juha Ahokas and Alvar Braathen for providing additional aerial photographs of the study area. And last, but certainly not least, to my better half Line and our dog Rapp for keeping me grounded throughout all of this.

Chapter 1

Introduction

1.1 Background

This thesis is a part of the project "Lower Cretaceous in the Arctic" (LoCrA), a joint effort led by the University Centre on Svalbard (UNIS) and the University of Stavanger, in collaboration with the University of Oslo, the University of Bergen and several international universities with backing from the petroleum industry. The project seeks to improve our understanding of the Lower Cretaceous knowledge of basin configuration, infill and structure of the Lower Cretaceous basins in the high Arctic, in order to better evaluate coarse siliciclastic wedges as plays on the Norwegian Continental Shelf.

1.2 Aims of study

This thesis aims to improve our understanding of the deformation structures of the area around Forkastningsfjellet, Spitsbergen, Svalbard, in particular to differentiate between Cenozoic and post-glacial structures. Previous structural studies of the area are few, limited to 2 geological maps and their associated commentary, and as such the field work undertaken for this thesis was exploratory in nature. The aim of the project was from the onset twofold; investigate and provide a model of formation for

the post-glacial landslides visible from Isfjorden, and conduct mapping of any Cenozoic deformation structures in the area. The landslide structures will be evaluated on both large-scale and individual fault block-scale, and possible stratigraphical controls on deformation will be discussed.

1.3 Methods

1.3.1 Field work and presentation of data

Field work for this thesis was carried out over the span of 3 weeks in late July and early August 2015. The field work was focused on the north-western slope of Forkastningsfjellet as well as Revneset north of Hanaskogelva. General morphological elements were measured, sketched and photographed, and structural data was gathered using a clinometer compass and GPS measurements. Strike- and dip measurements were taken using the right-hand rule, and averaging out 10-15 measurements. Remote approximate measurements were taken where the relevant structures were unreachable due to dangerous terrain.

1.3.2 Aerial photography

Digital, georeferenced ortophotographs (UTM zone 33N) were obtained from the Norwegian Polar Institute. Additional aerial photographs were supplied by Professor Alvar Braathen. Digital elevation models (DEM) for use in spatial analysis were obtained from the Norwegian Polar Institute.

1.3.3 Software

Georeferencing of field data and spatial analysis has been carried out in ESRI's ArcMap 10. ArcMap's spatial analyst and 3D analyst tools have been used to construct slope gradients and terrain profiles. Digital editing of field photographs and figuers have been accomplished using Adobe

Photoshop CS6. Stereoplots of field data have been created in Stereoplot 9 (www.geo.cornell.edu/geology/faculty/RWA/.../stereonet.html). MiKTeX 2.09 (miktex.org) has been used for word processing and layout.

1.3.4 Maps

A topographical base layer map shapefile for use in ArcMap 10 was obtained from the Norwegian Polar Institute. Geological maps from Major(Major 1964) and the Adventdalen C9G (Dallmann et al. 2000) map were used for comparison purposes.

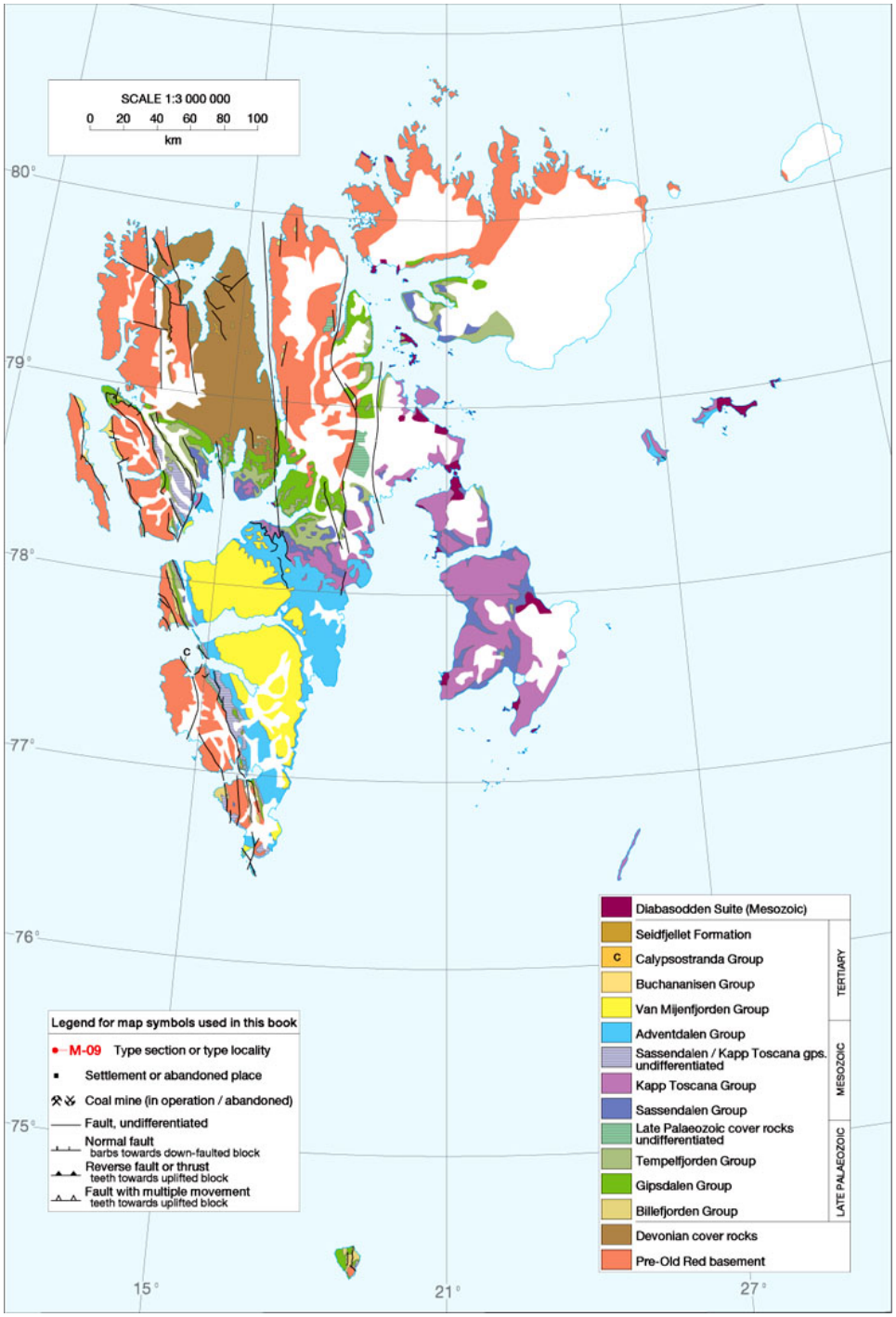

Figure 1.1: Geological overview map of the main lithostratigraphic units of Svalbard (Dallmann et al. 1999)

Chapter 2

Geological setting

2.1 Overview

The archipelago of Svalbard (Fig. 1.1), located in the High Arctic, represents the uplifted and exhumed western part of the Barents Sea Hydrocarbon Province. Uplift of Svalbard is considered due to two different uplift phases; a Jurassic to Cenozoic exhumation of northern Svalbard as the Amerasian basin opened, and uplift of western Svalbard during the Eocene to Oligocene Eurekean orogeny (Gasser 2013). The degree of uplift and exhumation was largest in the northern and western regions of Svalbard, and subsequent erosion exposed the oldest rocks on Svalbard in these regions. Svalbard consists of several islands, of which Spitsbergen, Nordaustlandet and Edgeøya are the largest.

The bedrock geology of Svalbard consists, in broad terms, of a (1) Proterozoic to Middle Silurian crystalline basement, variably deformed and metamorphosed, overlain by (2) Devonian Old Red sandstones, (3) Upper Paleozoic clastic sedimentary- and carbonate deposits, (4) Mesozoic deep marine, coastal and marginal marine clastic deposits, (5) Cenozoic clastic sedimentary deposits and (6) Quaternary volcanics (Dallmann et al. 1999).

Svalbard can be divided into 5 main lithotectonic units; the pre-Devonian

basement of western Spitsbergen and Nordaustlandet, the Devonian grabens of northern Spitsbergen, the Central Spitsbergen Basin, the platform areas of eastern Spitsbergen, and the West Spitsbergen Fold- and Thrust Belt (WSFTB) (Dallmann et al. 1999).

2.2 Major tectonic events

2.2.1 Pre-Caledonian tectonic history

Svalbard's pre-Caledonian tectonic history can, according to Gasser (2013), be broadly divided into 5 main stages; Paleoproterozoic arc accretion and extension (1), a Late Mesoproterozoic period of tectonic quiescence and sediment accumulation (2), Early Neoproterozoic active margin magmatism (3), Neoproterozoic to Palaeozoic rifting and passive margin development (4) and Late Neoproterozoic orogeny with localized Timanian fragments (5) (Gasser 2013). Due to Caledonian overprinting, these stages are not all present in all 3 (Fig. 2.1) basement provinces. The Northeastern terrane (Eastern basement province in Fig. 2.1) contains traces of stages 1, 2, 3 and 4, while stage 5 is only present in the Western terrane of southwestern Spitsbergen (Western basement province in Fig. 2.1) (Gasser 2013).

2.2.2 Caledonian orogeny

The Caledonian deformation history of Svalbard contains 3 principal events, spanning from the Lower Ordovician to the Devonian. Lower to Middle Ordovician HP metamorphism and magmatism (1), is mainly present in the Vestgötabreen and Richarddalen complexes on Svalbard. Widespread Silurian partial melting and magmatism (2) can be found in northwestern Spitsbergen and Nordaustlandet. Devonian to Carboniferous post-collisional extensional tectonics (3), led to the creation of half-graben basins for Old Red Sandstone (ORS) deposition (Gasser 2013).

2.2.3 Svalbardian deformation

The Svalbardian Fold- and Thrust belt of Latest Devonian/Earliest Carboniferous age is interpreted to represent a continuation of the Ellesmerian Fold Belt in North Greenland (Piepjohn 2000). During the Svalbardian deformation the ORS deposits of the Andrée Land Group, as well

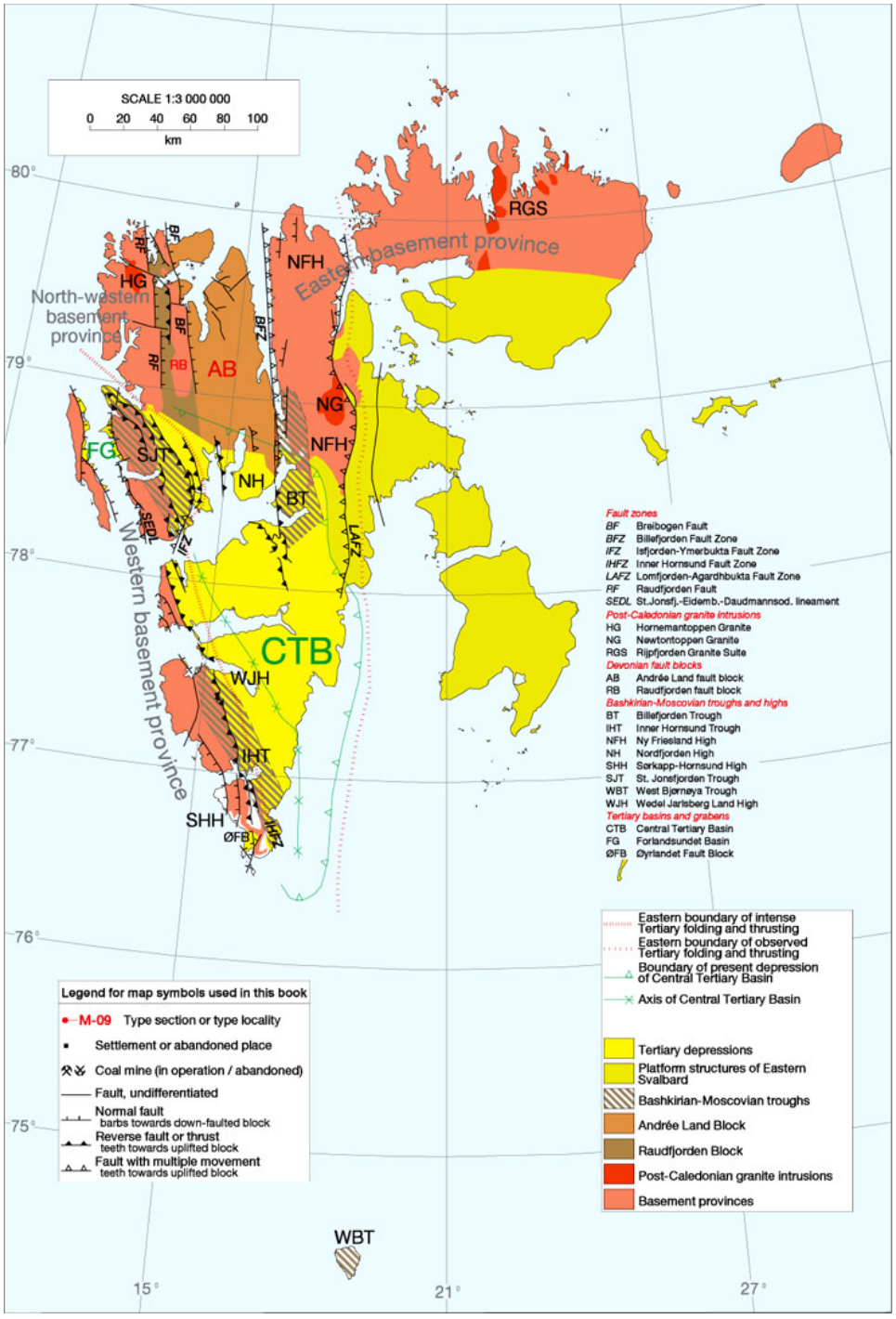

Figure 2.1: Overview map of the main pre-Devonian structural elements of Svalbard (Dallmann et al. 1999)

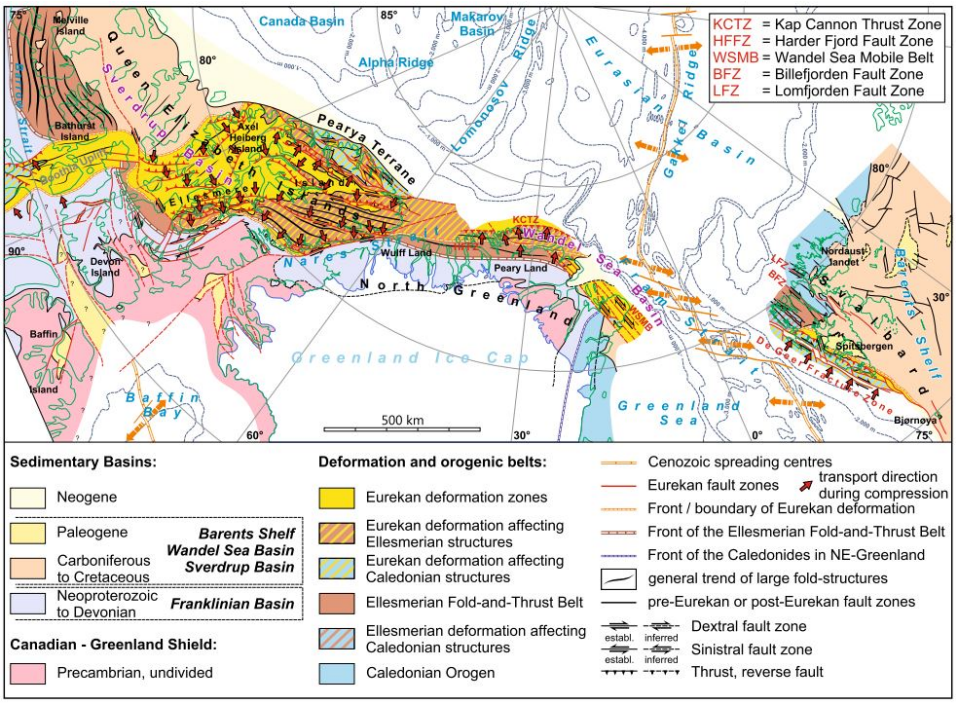

Figure 2.2: Tectonic map of the Eurekan, Ellesmerian and Svalbardian Fold- and Thrust Belts on Ellesmere Island, North Greenland and Svalbard (Piepjohn et al. 2015)

as the pre-Devonian basement, underwent west-vergent folding and west-directed thrusting (Piepjohn 2000). The dominant structural grain of the Svalbardian deformation is N-S, while the dominant structural grain of the Ellesmerian deformation (Fig. 2.2) on northern Greenland (E-W) and Ellesmere Island (E-W in the west, N-S in the south), varies (Piepjohn et al. 2015). This change in trend is not well understood.

2.2.4 Middle Carboniferous rifting

While there is some discussion regarding the exact boundaries between pre- and syn-rift deposits, the rift basin infill of the Billefjorden Trough can be divided into pre-rift (pre-Devonian basement, ORS deposits), syn-rift (Billefjorden Group and Lower Gipsdalen Group) and post-rift (Upper Gipsdalen Group and Tempelfjorden Group) successions (Dallmann et al. 1999; Maher and Braathen 2011).

2.2.5 Cenozoic shortening and extension

The Cenozoic deformation on Svalbard, linked to the Eurekan deformation in Northern Canada and North Greenland, is characterized by thin-skinned fold- and thrust-belt development and inversion of the Carboniferous rift basins (Piepjohn et al. 2015; Haremo et al. 1993).

The Paleocene to Eocene West Spitsbergen Fold- and Thrust Belt formed at a dextral transform margin between Greenland and Svalbard during the opening of the North Atlantic Ocean (Maher et al. 1995). The 175 km wide orogen is located on the western margin of Spitsbergen and is bounded by foreland blocks to the east. The WSFTB can be divided into 3 main structural areas; (1) an uplifted fold-thrust complex of pre-Devonian basement and Paleozoic cover rocks in the west, (2) a central zone of late Paleozoic-Cenozoic sedimentary cover with thin-skinned deformation, and (3) an eastern zone with a frontal duplex and flat-lying strata bounded by steep, reverse faults (BFZ and LFZ) (Bergh et al. 1997).

The development of the WSFTB can be divided into 5 stages: early Paleocene N-S contraction oblique to the orogen (stage 1) , major Eocene WSW-ENE contraction normal to the orogen (2), localized orogen-parallel transcurrent faulting (3), localized orogen-oblique transtension and transpression (4), and localized orogen-normal and orogen-oblique extension during an overall transtensional setting in the Oligocene (5) (Braathen et al. 1999). Total crustal shortening in the WSFTB is believed to be in the tens of km range (Bergh et al. 1997; Worsley 2008).

2.3 Geology of the pre-Devonian terranes

The pre-Devonian basement of Svalbard consists of Proterozoic, Cambrian, Ordovician and Silurian rocks. This assemblage was originally termed Hecla Hoek by Nordenskiold (1863) (Worsley 1986; Harland and Wilson 1956), a term no longer in use. Early investigation into the pre-Devonian basement assigned these rocks to a single metasedimentary succession (the Hecla Hoek Geosyncline) that predated the Caledonian orogeny (Gasser 2013).

The pre-Devonian crystalline basement of Svalbard can be divided into 3 main terranes; the Northwestern, Northeastern and Western terranes, owing to the occurrence of pre-Devonian rocks on Nordaustlandet, Ny Friesland, and along the Northwestern and Western coast of Spitsbergen (Fig. 1.1) (Gasser and Andresen 2012). The Northwestern and Northeastern terranes are similar, containing Mesoproterozoic sedimentation, Lower (950 Ma) Neoproterozoic granitic magmatism, and Neoproterozoic to Ordovician sedimentation, altered by Scandian phase magmatism and metamorphism. The Western terrane, in contrast, contains a Mesoproterozoic magmatic complex, Upper Neoproterozoic metamorphism and a Lower- to Middle Ordovician blueschist-to-eclogite facies metamorphic complex, as well three distinct unconformities of Neoproterozoic, Cambrian and Ordovician age. The Western terrane does not contain any evidence of Scandian phase magmatism or metamorphism (Gasser and An-

dresen 2012).

Amalgamation of the Northwestern and Northeastern terranes are thought to originate from the Northeastern margin of Laurentia, emplaced during the Caledonian orogeny (Gee et al. 2008). These terranes are bounded by large-scale, transcurrent, N-S striking faults, with predominantly strike-slip kinematics. The Western terrane, appearing undeformed by Scandian phase deformation, was most likely located north of Greenland during the main phase of the continent-continent collision (Gasser and Andresen 2012).

2.4 Devonian basin development

Paleomagnetic reconstructions place Svalbard around the equator during Devonian time (Torsvik et al. 2002). From the Upper Silurian to the Lower Devonian a several kilometer-thick unit of Old Red Sandstone (ORS) was deposited in a major post-Caledonian graben in Northern Spitsbergen, with sediments mainly derived from the orogen (Worsley 2008). The ORS deposits are bounded by the NW and NE basement provinces (Dallmann et al. 1999). The shift from the red ORS deposits to the grey fluvial sedimentation in the upper part of the Andrée Land group indicates a change from arid to tropical climates and eustatic sea level change as Svalbard moved towards the equator (Worsley 2008).

2.5 Lower Carboniferous pre- and syn-rift deposits

The Billefjorden Group consists of grey sandstones, shales and conglomerates, with localized coal seams, indicating a warm, humid depositional environment consistent with Svalbards location in the tropics (Dallmann et al. 1999). As syn-rift deposits, the Billefjorden Group was not confined to the rift basins (fig 2.4), but it is there that it has been preserved (Dallmann et al. 1999).

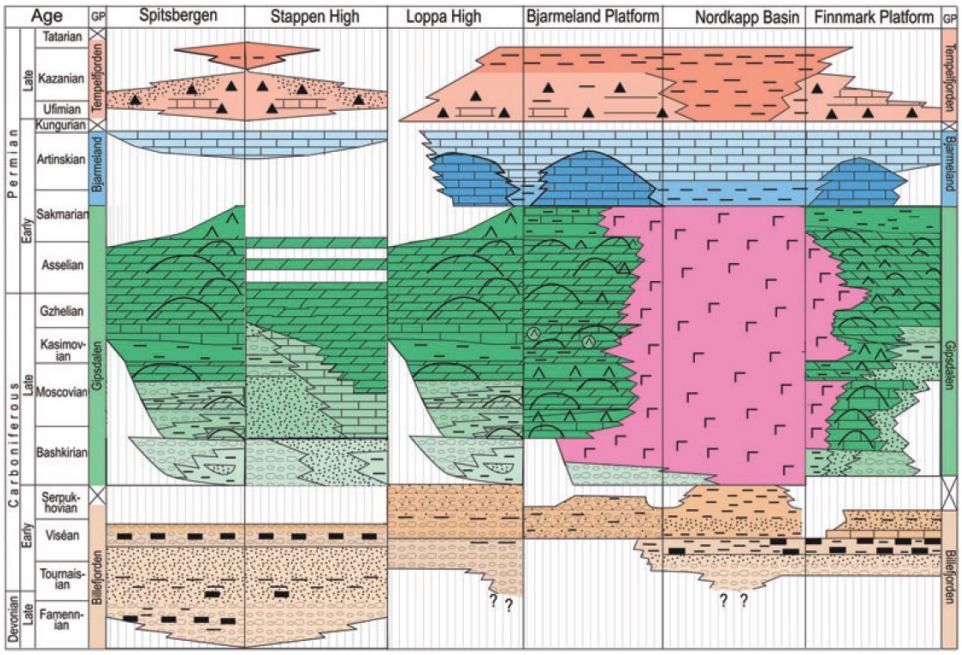

Figure 2.3: Upper Palaeozoic Lithostratigraphy of the Barents Sea, including Svalbard (Worsley 2008)

Following the Svalbardian deformation, extensional reactivation of the Billefjorden Fault Zone and regional uplift led to the creation of rift basins in Spitsbergen, particularly the Billefjorden Trough (Haremo et al. 1990; Bælum and Braathen 2012). These newly formed basins and their faulted margins created accommodation space, and provided a source of clastics, for the syn-rift sediments of the Gipsdalen Group to be deposited (Worsley 2008).

Deposited following a Middle Carboniferous hiatus, the lower part of the Gipsdalen Group is dominated by clastics (syn-rift), while the later successions contain mainly evaporites, carbonates and red mixed clastics (post-rift), consistent with fluvial to alluvial environments in in a warm, arid climate (Dallmann et al. 1999).

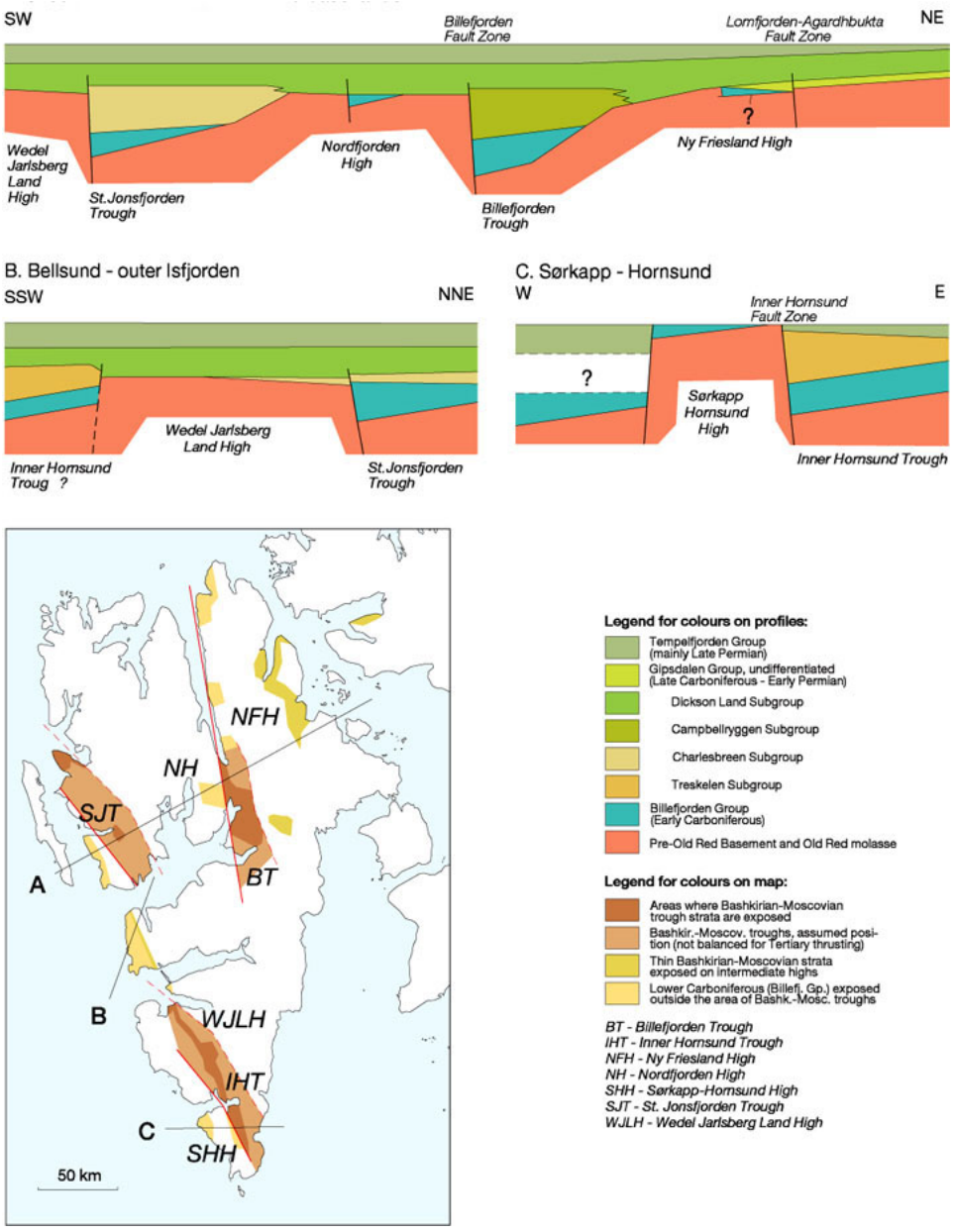

Figure 2.4: Middle Carboniferous troughs and highs (Dallmann et al. 1999)

2.6 The Upper Carboniferous-Permian carbonate platform

As Laurussia drifted northwards during the Upper Carboniferous, Svalbard moved into the subtropics (Torsvik et al. 2002). A period of tectonic quiescence accompanied by a transgression related to the melting of the Gondwanan ice cap provided a stable carbonate platform and marks the end of the Gipsdalen Group and the start of the Bjarmeland Group (Worsley 2008).

The Lower to Middle Permian Bjarmeland Group consists of cool-water carbonates deposited after a major flooding event. This group is only present on southern Spitsbergen (Sørkapp and Hornsund) on mainland Svalbard (Worsley 2008; Dallmann et al. 1999).

Deposited in the Middle to Upper Permian, the post-rift Tempelfjorden Group overlies a significant subaerial erosional surface and represents a shift to cooler climates following a regional transgressional event as rifting opened a passage from the Boreal Sea to the North Sea (Worsley 2008; Dallmann et al. 1999). Cherts, siliceous shales, sandstones and limestones represent deep marine facies conditions under which the Tempelfjorden Group was deposited (Worsley 2008).

A dramatic change, following a widespread hiatus, from the cold-water deep marine facies of the Tempelfjorden Group to the warm-water facies of the Sassendalen Group represents a significant sea-warming event and might be a contributing cause to the end-Permian mass extinction event (Worsley 2008).

2.7 Mesozoic silisiclastic deposits

By the advent of the Mesozoic era, Svalbard was situated at the shelf on the northern edge of Pangaea at about 45 degrees north. By the end of the Mesozoic, Svalbard had drifted to roughly 65 degrees north (Torsvik et al.

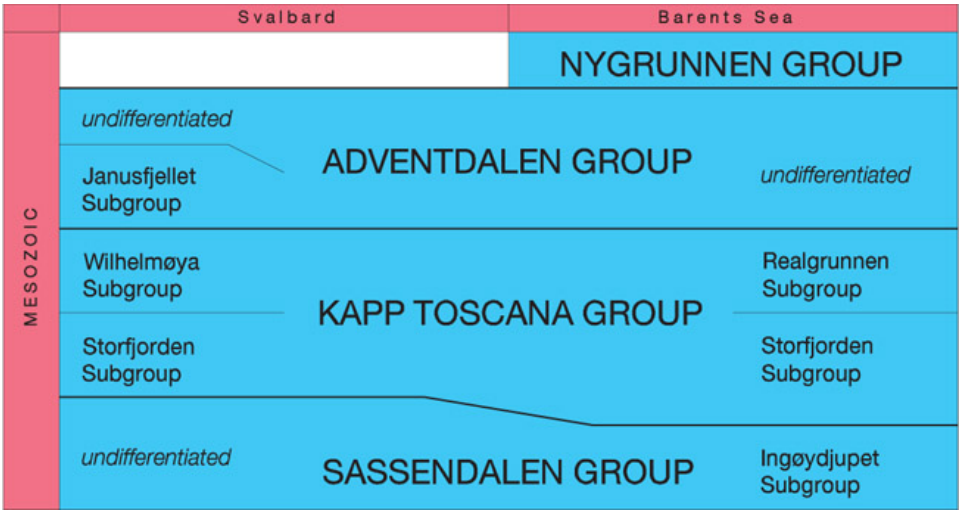

Figure 2.5: Mesozoic lithostratigraphy on Svalbard and in the Barents Sea (Dallmann et al. 1999)

2002). A stable tectonic setting combined with cyclical variations in sea level produced the Sassendalen Group, a series of stacked transgression-regression successions of shelf and deltaic deposits (Dallmann et al. 1999).

As Svalbard continued to drift northwards, a change from dry to wetter climatic conditions combined with a local regression, and Svalbard shifting from a coastal setting to an epicontinental sea setting, resulted in the deposition of the Kapp Toscana Group in the late Triassic. The Kapp Toscana Group consists of shales, siltstones and sandstones of Upper Triassic to Middle Jurassic age (Dallmann et al. 1999).

Following a significant Middle Jurassic transgression, the deltaic to deep marine deposits of the Lower Adventdalen Group (Janusfjellet Subgroup) were formed (Dypvik et al. 2002). The lower part of the Janusfjellet Subgroup (Agardhfjellet Formation) is mainly comprised of black bituminous shales (Dallmann et al. 1999).

The incipient breakup of Pangaea in the Middle Jurassic marks the end of a long period of tectonic quiescence in Svalbard. Northward propagation of the Atlantic sea-floor spreading axis led to widespread rifting and reactivation of pre-existing faults, reaching its most intense activity in the

Late Jurassic (Worsley 2008). A Late Jurassic meteor impact created the Mjølninr crater of the Barents Sea, and may have also contributed to the change in depositional environment (Worsley 2008).

A regional fall in sea level created a shift from an anoxic, black shale-producing depositional environment to more open marine conditions at the Jurassic/Cretaceous boundary Worsley 2008. The Lower Cretaceous part of the Adventdalen Group (Rurikfjellet, Helvetiafjellet and Carolinefjellet formations, detailed in section 3.2) is dominated by clastics; shales, mudstones, sandstones and conglomerates (Dallmann et al. 1999). A warm and humid climate facilitated the growth of coniferous forests, peatlands and dinosaur populations (Nemec 1992).

As Laurasia split into Eurasia and North America during the Cretaceous, widespread rifting and volcanic activity added basaltic flows to the Adventdalen Group (Kong Karls Land flows) (Dallmann et al. 1999). Significant uplift and subsequent erosion in the Middle to Upper Cretaceous give rise to an unconformity between the Lower Cretaceous Adventdalen Group and overlying Cenozoic rocks (Worsley 2008).

2.8 Cenozoic deposits

The Lower Cenozoic rocks of the Van Mijenfjorden Group (Fig. 2.6) are mainly preserved in the Central Spitsbergen Basin and Ny-Ålesund (the Ny-Ålesund Subgroup) as well as in a separate basin between western Spitsbergen and Prins Karls Forland, the Forlandssundet Graben (Dallmann et al. 1999; Worsley 2008). The sandstones, siltstones and shales in the Van Mijenfjorden Group are of Paleocene to Oligocene age, sourced from the Cenozoic orogen West Spitsbergen Fold- and Thrust Belt, and deposited in a foreland basin setting (Dallmann et al. 1999). The Buchananisen Group of Forlandssundet (fig 2.6) post-date the West Spitsbergen Fold- and Thrust Belt (Dallmann et al. 1999).

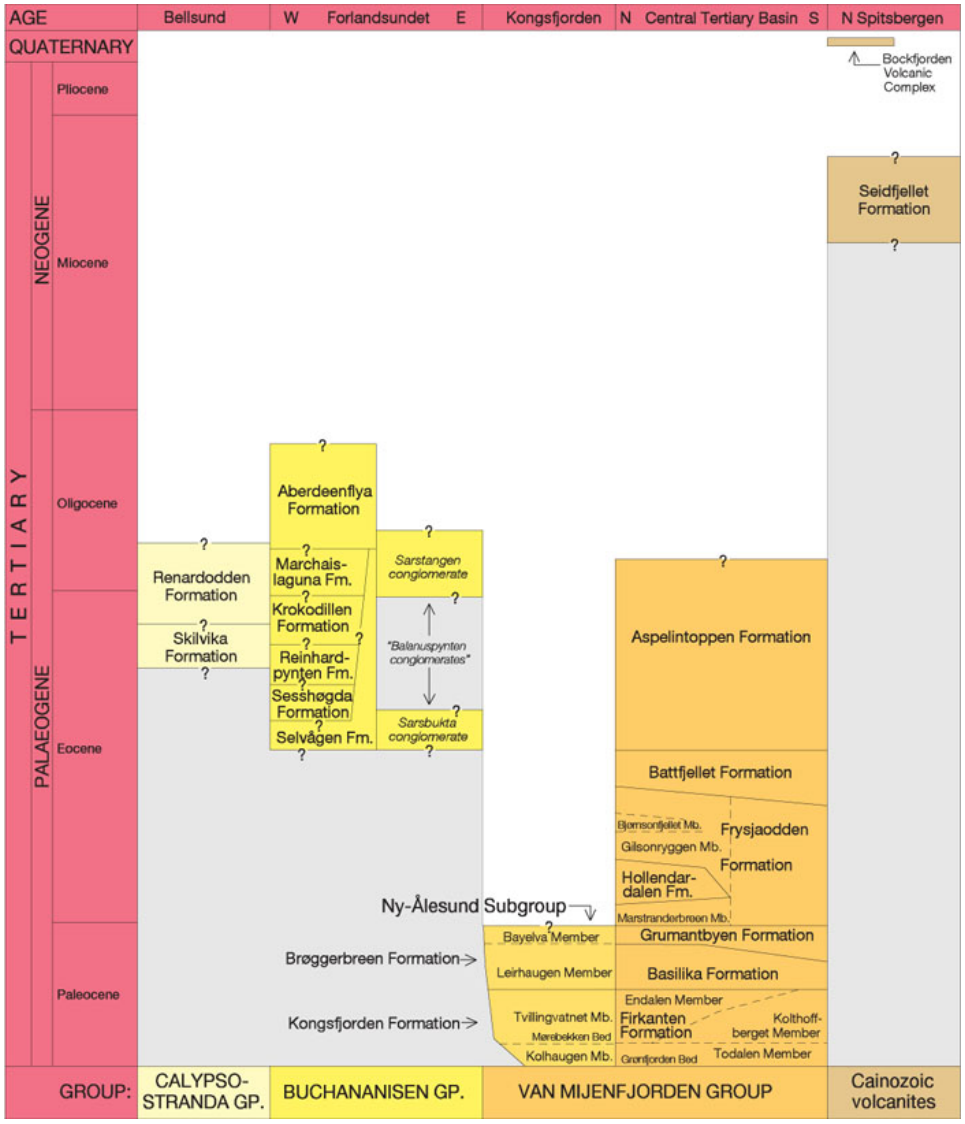

Figure 2.6: Cenozoic lithostratigraphy on Svalbard and in the Barents Sea (Dallmann et al. 1999)

2.9 Quaternary glacial deposits and volcanics

Throughout the Quaternary, Svalbard and the Barents Sea have been repeatedly covered by large ice sheets. Although there is evidence of sea ice build-up as early as Middle Miocene, extensive glacial coverage on Svalbard is thought to have initiated around 1.6-1.3 ma (Ingolfsson 2011). Erosional unconformities indicate at least 16 major glacial events during the Quaternary, with large erosional and depositional footprints (Solheim et al. 1996). Due to these glacial cycles, the Quaternary stratigraphy of Svalbard consists of loose, unconsolidated sediments and the volcanics and subvolcanics of the Bockfjorden Volcanic Complex (Dallmann et al. 1999). The last glacial maximum (LGM) in Svalbard was 25-10 ka BP (Mangerud and Svendsen 1992). The last glacial retreat in the Isfjorden area is thought to be along a N-S axis, towards the north (Forwick and Vorren 2010).

Chapter 3

Geology of Forkastningfjellet

3.1 Overview

Forkastningsfjellet, the study area, is located on the eastern edge of Isfjorden, across Adventfjorden from Longyearbyen airport. The area covers about 5.3 square kilometers, with a maximum elevation of 482 m.a.s.l. As the name suggests, the area has been heavily faulted, undergoing both shortening during the transpressional tectonic regime of the Cenozoic, as well as postglacial landsliding of the area proximal to Isfjorden.

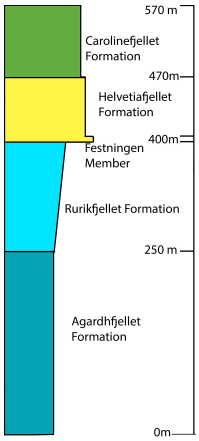

Figure 3.2: Simplified stratigrahical column for Forkastningsfjellet. Magnitudes from Braathen et al. 2012

Upper Jurassic to Lower Cretaceous rocks make up the lithostratigraphy of Forkastningsfjellet, of which the Rurikfjellet and Helvetiafjellet formations are the most prominent con-

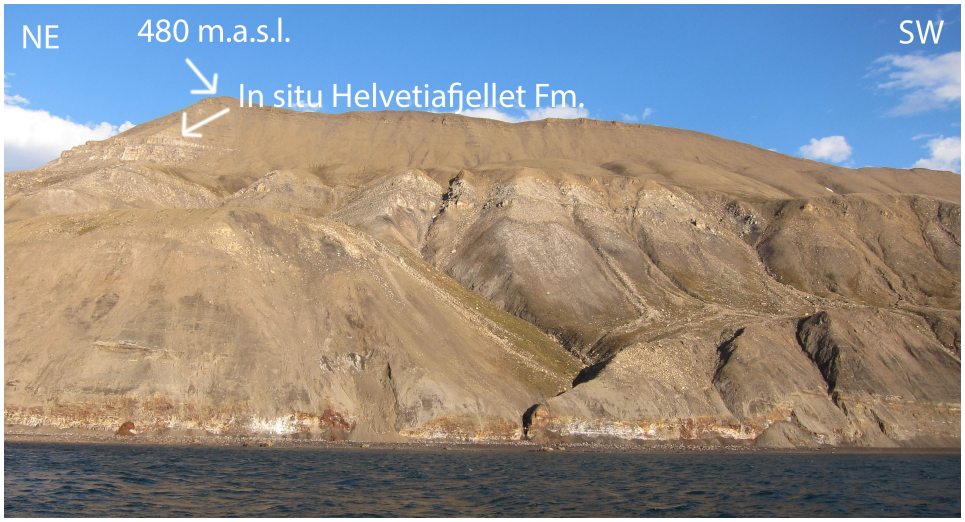

Figure 3.1: Northwestern slope of Forkastningsfjellet as viewed from Isfjorden. In situ Helvetiafjellet Formation in the upper left corner, downfaulted hanging wall blocks in the foreground.

stituents in this location. The strata in this location are generally subhorizontal, gently dipping towards the southeast.

3.2 Previous structural studies

Previous work on Forkastningsfjellet has focused on sedimentological (Grosfjeld 1992) and sequence stratigraphical investigations (Gjelberg and Steel 2012; Nemec et al. 1988; Midtkandal et al. 2007). No detailed structural studies have been published on Forkastningsfjellet, but some structural data are present on maps from Major (1964) and in the interpretation of the geology of the study area (Adventdalen map C9G)(Dallmann et al. 2000).

The two maps have some significant differences; a NW-striking, top-to-the-West thrust fault cuts the southern tip of Forkastningsfjellet in Major's 1964 map (Fig. 3.3), whereas the same structure has been interpreted to be a monoclinal fold in the most recent map (Fig. 3.4).The subdivision of landslide blocks in the area also differ between the two maps; Major has mapped 6 distinct blocks, while NPI's map contains only 3 blocks.

Figure 3.3: Map section of Forkastningsfjellet and the surrounding area. Modified from Major 1964

Figure 3.4: Map section of Forkastningsfjellet and the surrounding area. Modified from Dallmann et al. 2000

Figure 3.5: Light-colored siltstones amid black and shales of the Kikutodden Member of the Rurikfjellet Formation, Forkastningsfjellet

3.3 Lithostratigraphy

3.3.1 Rurikfjellet Formation

Deposited under open marine, oxygen-rich conditions, the mudstone-dominated Rurikfjellet Formation of the upper Janusfjellet Subgroup displays a general upward shallowing trend of shore-face and delta lobe deposits (Midtkandal et al. 2007).

The upper part of the Rurikfjellet Formation, referred to as the Kikutodden Member (Midtkandal et al. 2008), consists of upwards coarsening successions of grey to black shales, mudstones, siltstones and sandstones, bounded by flooding surfaces (Fig. 3.5). The number of parasequences vary by location, anywhere from 1 to 5 successions have been observed (Dypvik 1991), but only 2 are present in the study area. The parasequences display a general aggradational trend, with a stacked regressive parase-

quence set (Midtkandal et al. 2008).

3.3.2 Helvetiafjellet Formation

The Lower Cretaceous Helvetiafjellet Formation is generally regarded as bipartite, with a thick sandstone succession at its base, followed by a heterolithic succession. It displays significant thickness variations, within a range for 40-155 m (Dallmann et al. 1999). A regional erosional unconformity is generally regarded as its base and separates the Helvetiafjellet Formation from the underlying Rurikfjellet Formation (Nemec et al. 1988; Midtkandal et al. 2008). The sheet-like sandstones of the Festningen Member (Fig. 3.6) are thought to represent fluvial deposits from a braided river systems deposited at the onset of the Helvetiafjellet Formation. A thin, basal fluvial conglomerate bed with poorly sorted and well rounded clasts marks the start of the sequence (Midtkandal et al. 2008).

Overlying the Festningen Member is the heterolithic Glitrefjellet Member of the Helvetiafjellet Formation. The Glitrefjellet Member displays a wide variety of facies associations within a deltaic to fluvial channel setting (Midtkandal et al. 2007). Coarse, grey, cross-bedded and ripple-laminated sandstones interweave with organic-rich shales and coal seams and display a conformable boundary to the overlying Carolinefjellet Formation (Dallmann et al. 1999). The massive sandstones of the Festningen Member are clearly visible in the landscape, even at a distance, and are as such useful as marker layers for identifying faulted sections.

3.3.3 Carolinefjellet Formation

Deposited in a prodeltaic to marine shelf setting, the Carolinefjellet Formation displays alternating beds of shales and sandstones. Formed as a response to a transgression following the paralic conditions of the Helvetiafjellet Formation (Dallmann et al. 1999; Midtkandal et al. 2007), the sandstone-dominated lower part of the Carolinefjellet Formation

Figure 3.6: Festningen Member sandstone, Forkastningsfjellet

(Dalkjegla Member) contains fine-grained grey-greenish sandstones with occasional storm deposits (Dallmann et al. 1999).

Chapter 4

Results

4.1 General morphology

The study area can be roughly divided into terraces (flat areas) and ramps (steep slopes). Fig. 4.1 shows the distribution of these types of terrains. The northwestern side of Forkastningsfjellet itself consists of two steep ramps separated by a terrace. In general, the terraces are covered by vegetation and scree, while the ramps are well exposed. The southern section of Forkastningsfjellet does not display this morphology, consisting of just one ramp and one terrace.

The area is presently undergoing some mass movement; scree formation from small-scale rockfalls and rockslides were observed during field work.

4.2 Cenozoic structures

Cenozoic structures were separated from recent post-glacial structures by the presence of cementation and/or ductile deformation in fault cores and folds, as well as by stress regime. In general, Cenozoic structures are confined to the southern part of Forkastningsfjellet and further south.

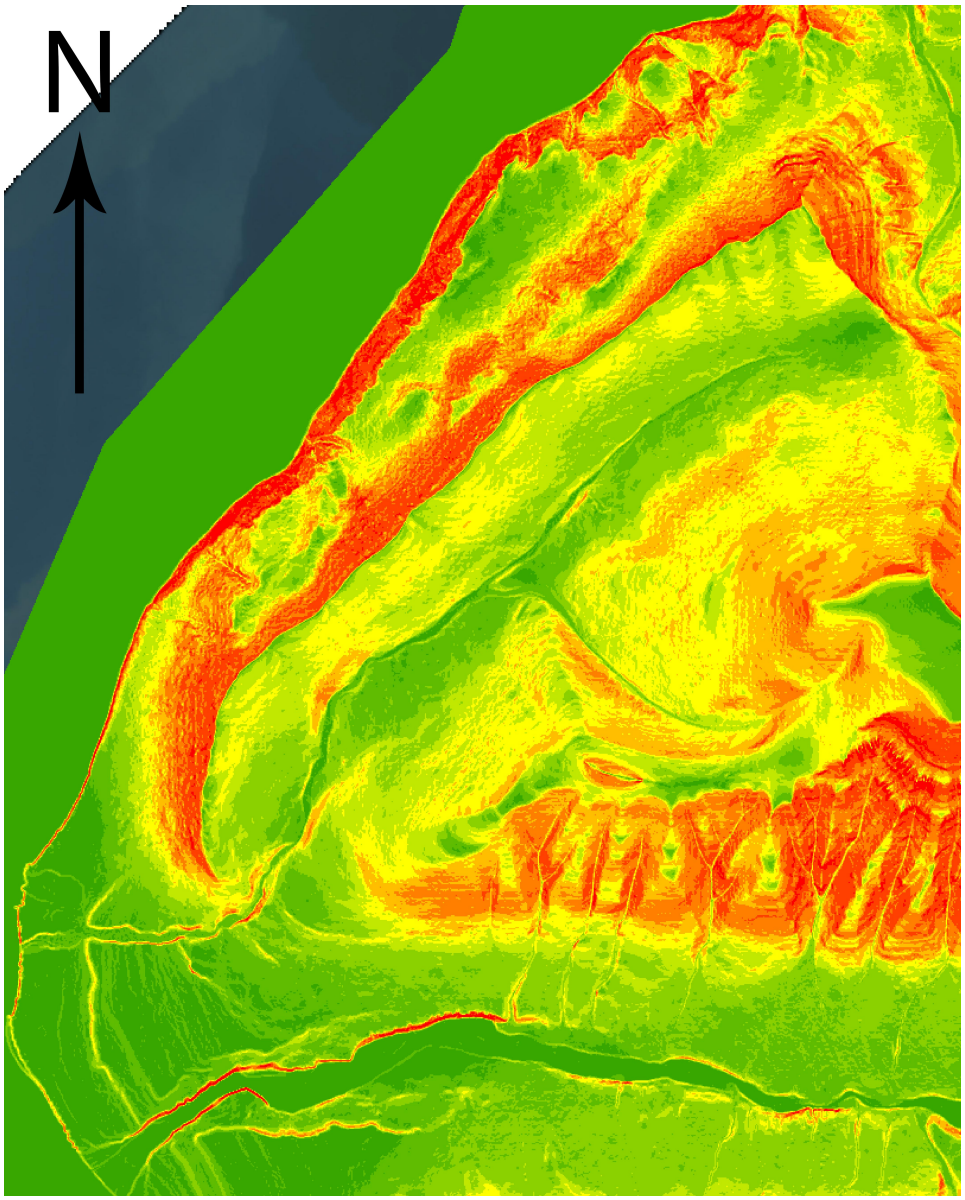

Figure 4.1: Slope distribution of the area around Forkastningsfjellet - from bright green (0-4 degrees) to bright red (45-79 degrees)

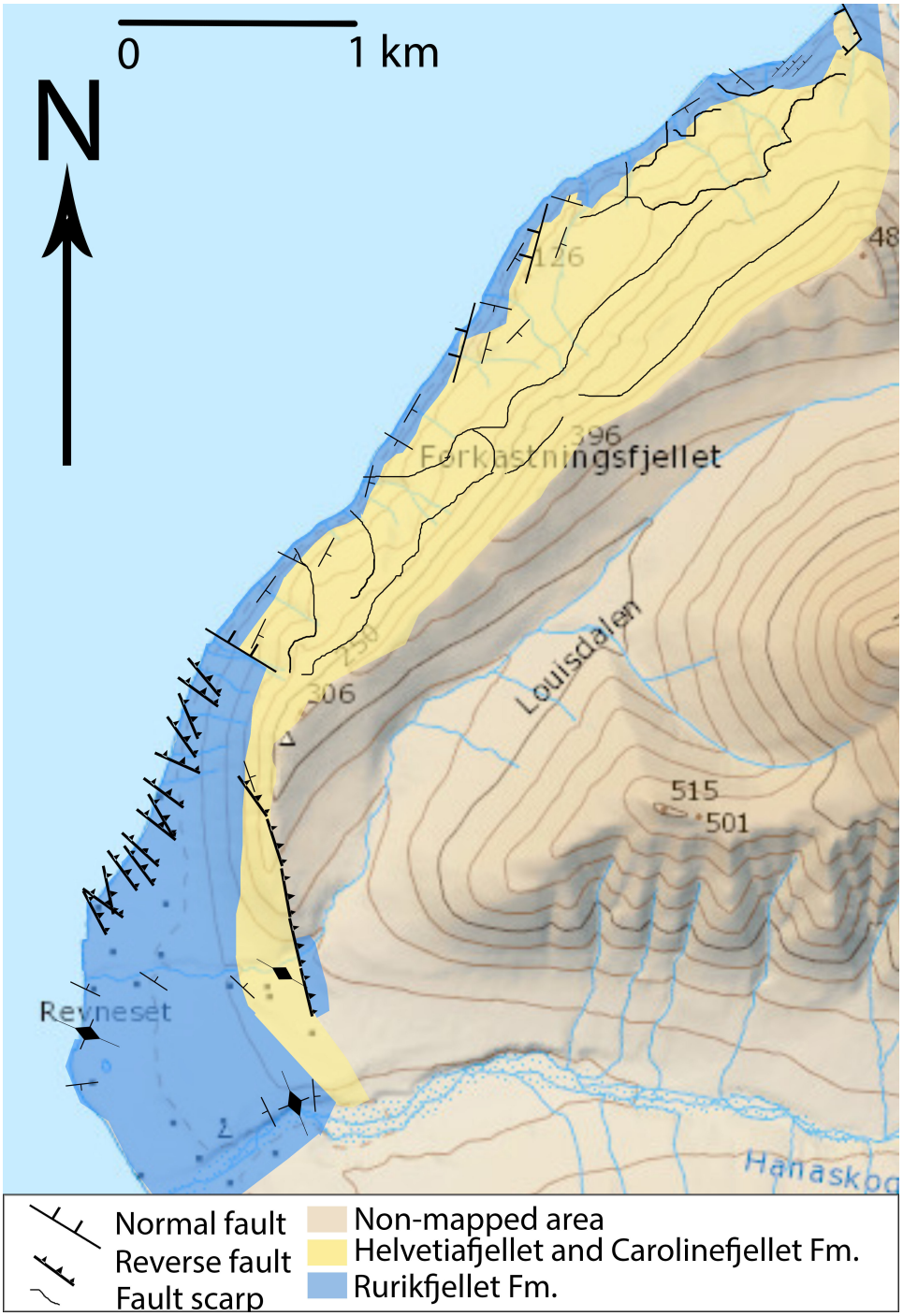

Figure 4.2: Structural map of the area around Forkastningsfjellet

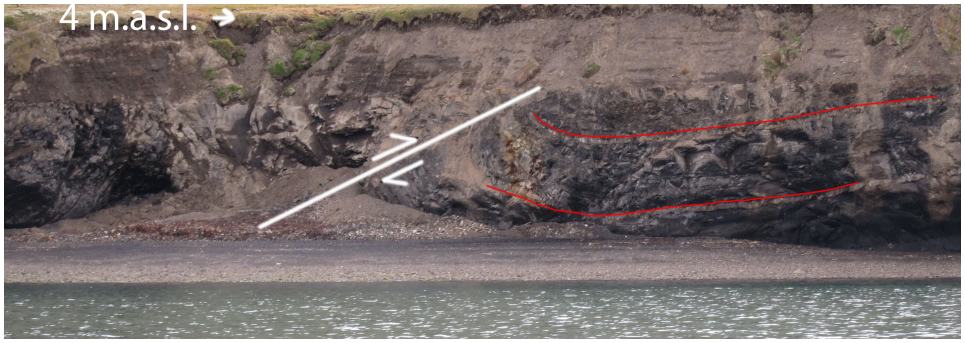

Figure 4.3: Reverse faulting in the Rurikfjellet Formation, Revneset. A drag fold is exposed in the footwall (red).

4.2.1 Compressional structures

The terrace north of Louisdalelva and the southern part of Forkastningsfjellet contain a set of NW-striking reverse faults (Fig. 4.2 and 4.4). Several smaller faults (<2 m throw) are located along the beach, while a larger fault (45 m throw) is found in the southern tip of Forkastningsfjellet. These smaller reverse faults are mostly steep, with dip angles ranging from 25 to 71 degrees, with the majority around 50 degrees. The major fault, here referred to as Revneset Reverse Fault (RRF) dips 30 degrees to the northwest (Fig. 4.5,4.6). As the RRF fault plane was measured remotely from a boat, there is a significant degree of uncertainty associated with this measurement.

Along the southeastern bank of Louisdalelva a reverse fault cuts the upper Helvetiafjellet Formation, thrusting the Kikutodden Member of the Rurikfjellet Formation on top of it (Fig. 4.7).

4.2.2 Folding and ductile deformation

Two anticlinal folds have been identified. A tight, NE-verging, NW-trending fault-propagation fold exposed in the Helvetiafjellet Formation by Louisdalelva (Fig. 4.7) and an open, upright, NNW-trending fold in the Rurikfjellet Formation exposed by Hanaskogdalelva (Fig. 4.2). The axial plane of a monoclinal fold by the power plant outside Longyearbyen was

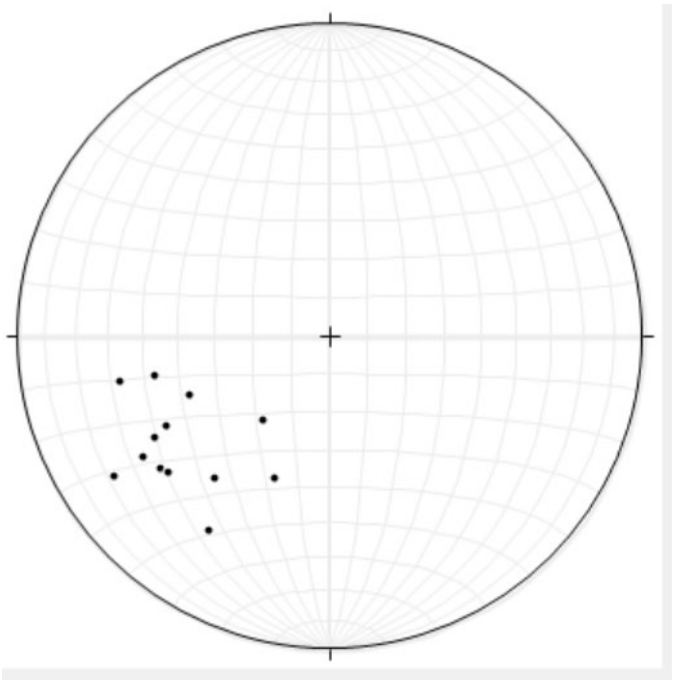

Figure 4.4: Stereoplot of poles to Cenozoic reverse faults at Revneset (Schmidt projection, lower hemisphere)

measured to 033/55 for comparison purposes. A third, WNW-trending antiform can be inferred from strike/dip variation in bedding planes along the coast north of Louisdalelva, but the hinge itself is not visible (Fig. 4.2).

Helvetiafjellet Formation, and in particular the Festningen Member, contain plentiful slickenlineations (Fig. 4.8). The slickenlineations indicate left-lateral, right-lateral and normal movement.

4.2.3 Extensional structures

No large-scale Cenozoic extensional structures have been identified in the study area. A normal fault exposed by the road to Longyearbyen airport was measured to 053/70 for comparison purposes. A WNW-striking normal fault separating the landslide-affected areas from the rest of the study area (Fig. 4.10) is exposed by the beach. Its fault core contains lithified lenses (Fig. 4.11) of Rurikfjellet Formation shale, but its age is

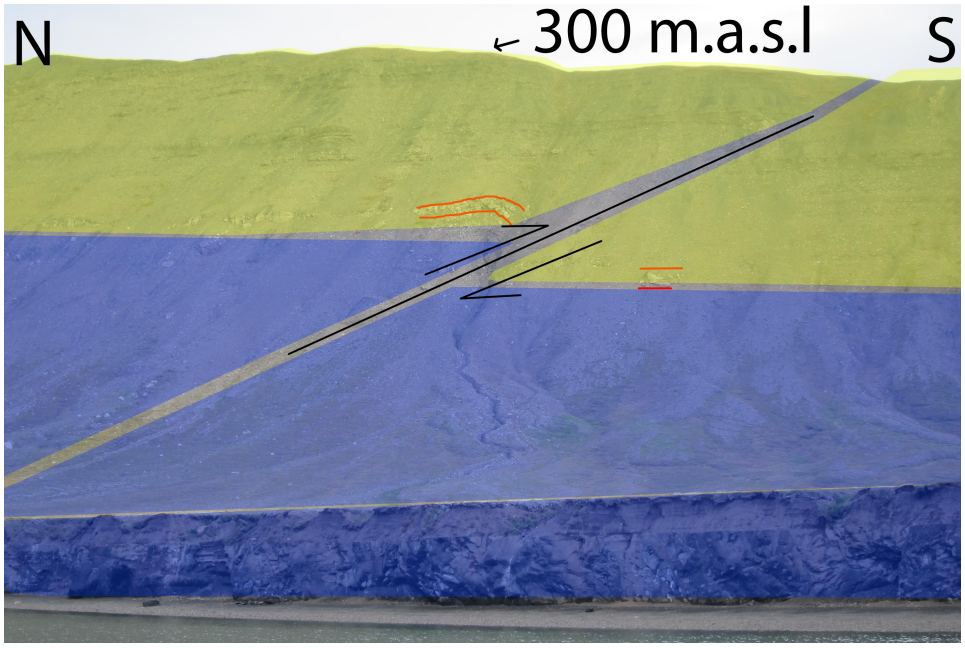

Figure 4.5: Revneset Reverse Fault, with a throw of 45m, superimposes upper Rurikfjellet Formation (blue) on Festningen Member (lower red marker layer). A drag fold in Festningen Member and the Carolinefjellet Formation can be seen on the hanging wall along the fault plane. Carolinefjellet and Helvetiafjellet Formations in yellow.

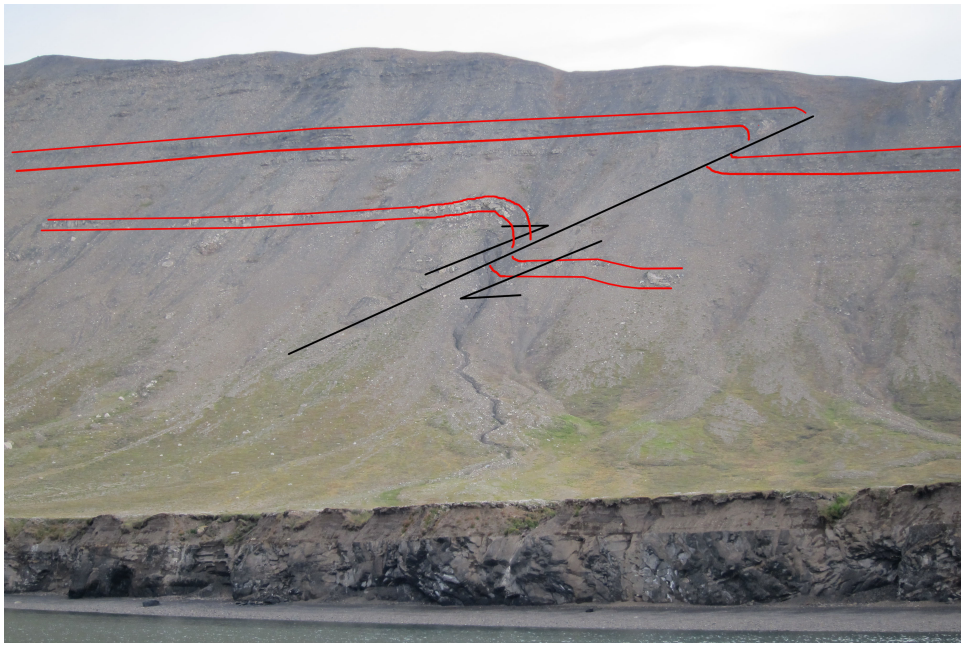

Figure 4.6: Revneset Reverse Fault

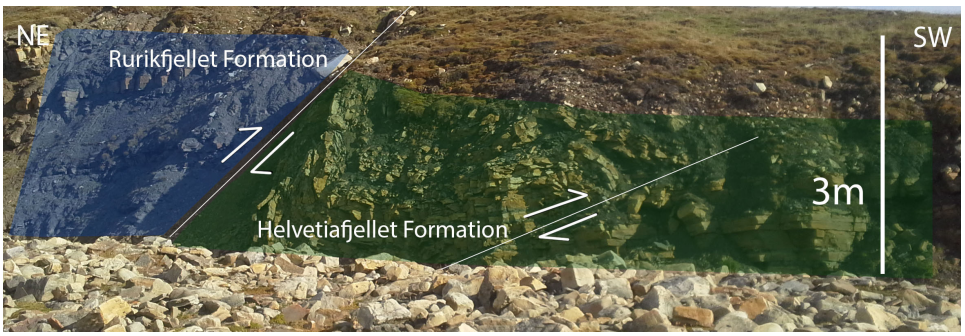

Figure 4.7: Reverse fault and fault-propagation folding on the SE bank of Louisdalelva.

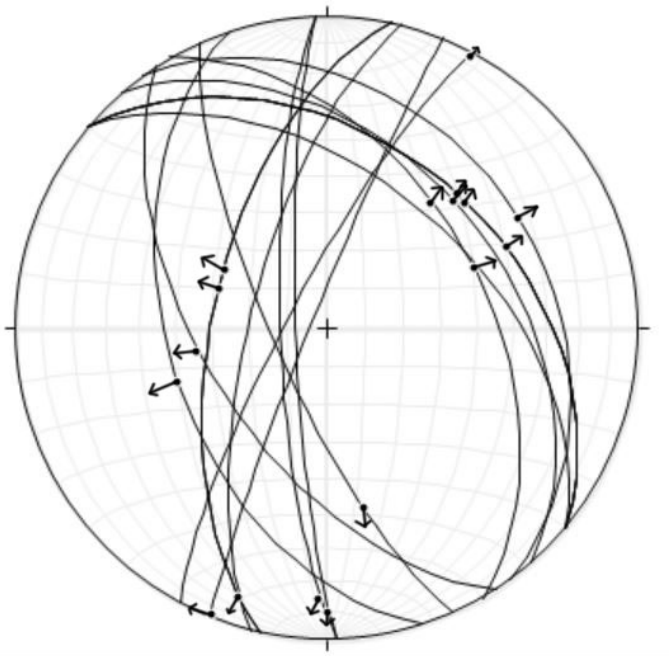

Figure 4.8: Stereoplot (poles and planes) of Cenozoic slickenlineations in the Helvetiafjellet Formation.

Figure 4.9: Slickenlineations in an in situ outcrop of the Festningen Member.

uncertain.

4.3 Summary

The majority of Cenozoic structural features in the study area are compressional, primarily in the form of top-to-the-WSW thrust faults. These structures are confined to the southern part of the study area, with no trace of Cenozoic deformation, outside of slickenlineations, in the northern part.

4.4 Post-glacial landslide structures

Post-glacial deformation was identified on the basis of an absence of ductile deformation, mineralization or cementation of fault rocks. As the terraces are mostly covered by scree and vegetation, fault scarps believed to separate ramps and terraces have been approximated in maps.

Figure 4.10: WNW-striking normal fault in the Rurikfjellet Formation.

Figure 4.11: Close-up of lithified fault core lense from Fig. 4.10

4.4.1 Large-scale structures and landslide blocks

Fault scarps identified on the basis of DEM-derived slope gradient plots and field observations generally belong to two sets; NE-striking scarps and NW-striking counterscarps. Individual fault blocks are thought to be separated by NW-striking listric normal faults, orthogonal to the NE-striking listric master faults (Fig. 4.2). Fault blocks display rotation of bedding planes towards the footwall (Fig. 4.12). From an in situ dip average of 5 degrees towards the ESE, fault blocks display additional bedding plane rotation from 15 to 35 degrees towards the footwall. In general, rotation of bedding planes appear to be uniform within a block, but one fault block displays a deviation from this trend (Fig. 4.14). Within this block, the Kikutodden Member of the Rurikfjellet Formation. has been rotated from its in situ dip of 5 degrees towards ESE, to 30 degrees towards ESE, a net rotation of 25 degrees towards the footwall. The Festningen Member has undergone a net rotation of 5 degrees. Roll-over anticlinal structures appear in the fault blocks, but these seem confined to upper Helvetiafjellet Formation and Rurikfjellet Formation, while Festningen Member appears to deform more rigidly within the same block (Fig. 4.13).

Most fault blocks display additional planar faulting on the distal tips of the hanging wall, leading to an apparant doubling of marker layers (Fig. 4.15) Planar faulting on this scale within the Helvetiafjellet Formation has only been observed on the exterior of the blocks, while possible analogous structures within the Rurikfjellet Formation have been observed in the interior of the blocks (Fig. 4.16).

Figure 4.12: Fault block rotated 35 degrees towards the hanging wall

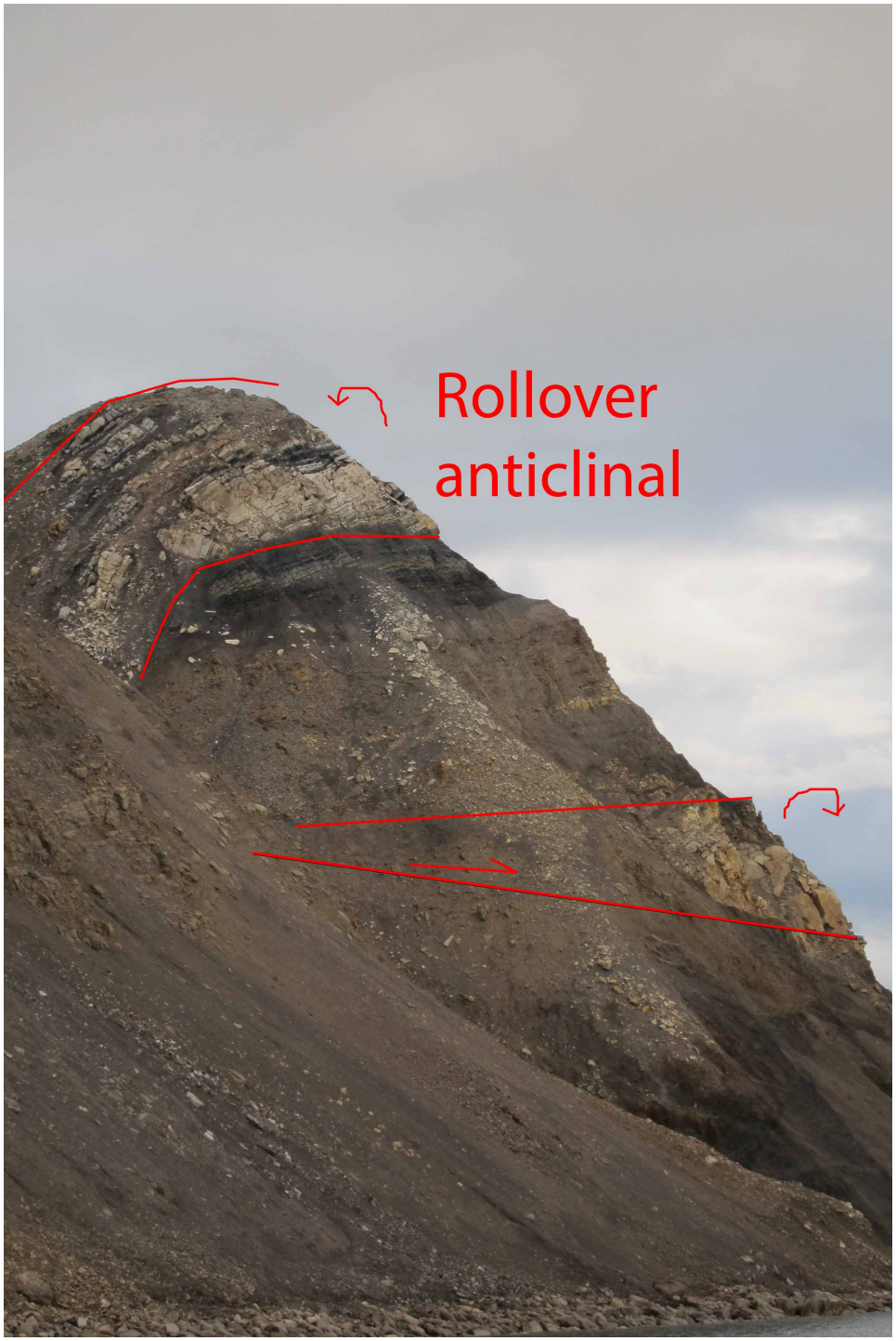

Figure 4.13: Roll-over anticline in upper Helvetiafjellet Formation fault block outcrop with non-folded Festningen Member

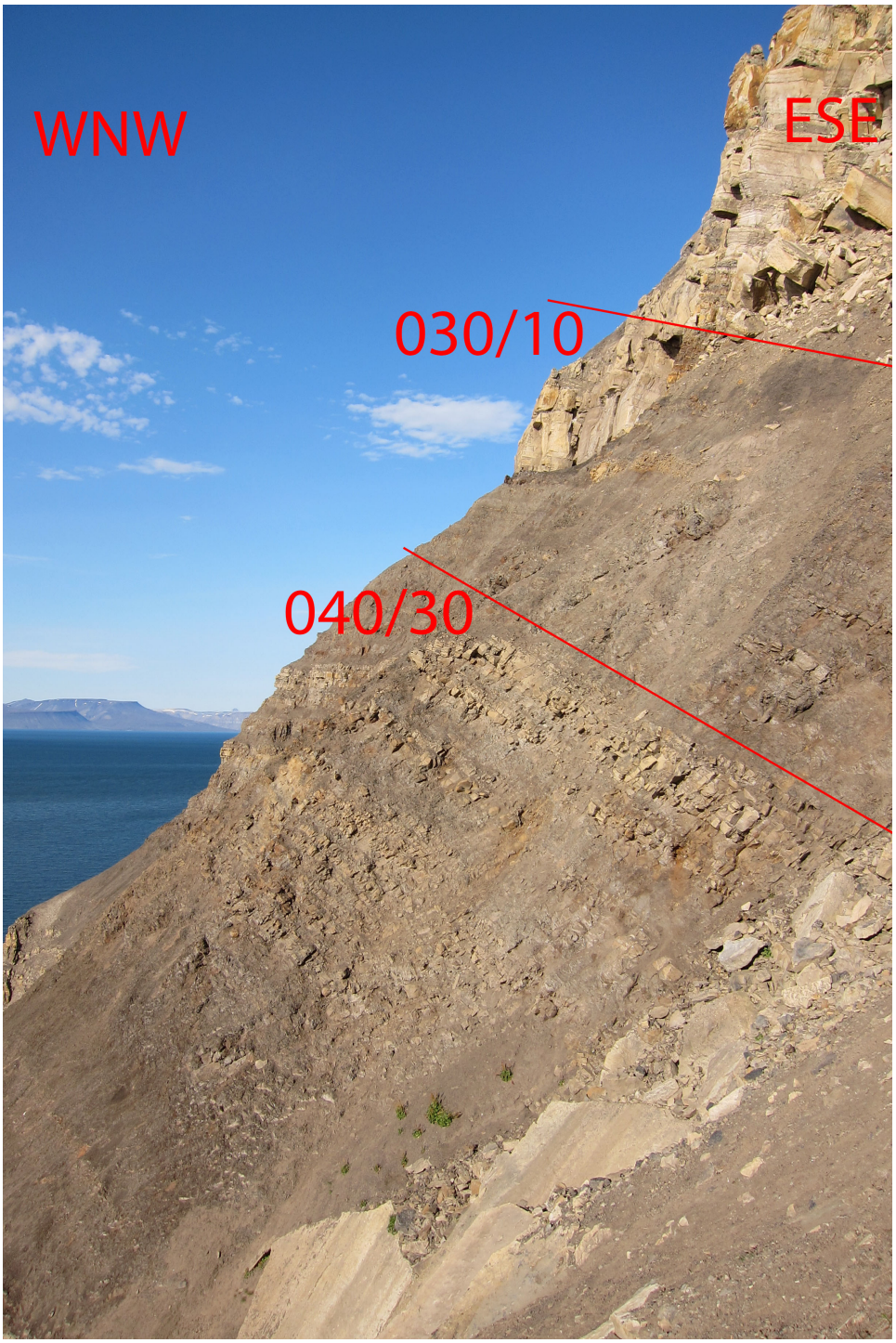

Figure 4.14: Fault block displaying non-uniform rotation of bedding planes

Figure 4.15: Planar faulting on the distal tips of the fault blocks leading to apparant doubling of sections (photo by Juha Ahokas)

4.5 Internal deformation structures

4.5.1 Rurikfjellet Formation

The shale-dominated parts of Rurikfjellet Formation deform by low-throw, high-angle normal faulting, striking parallel to the slope (Fig. 4.16). These fault cores contain mainly breccias and gouge, with no apparant lithification of fault rocks. The upper, siltier parts of Rurikfjellet Formation appears to develop 3 sets of fractures, with slope-parallel, slope-normal (Fig. 4.17) and slope-oblique fracture planes. These 3 sets of fractures are not present uniformly throughout the Kikutodden Member, but are localized in lenses.

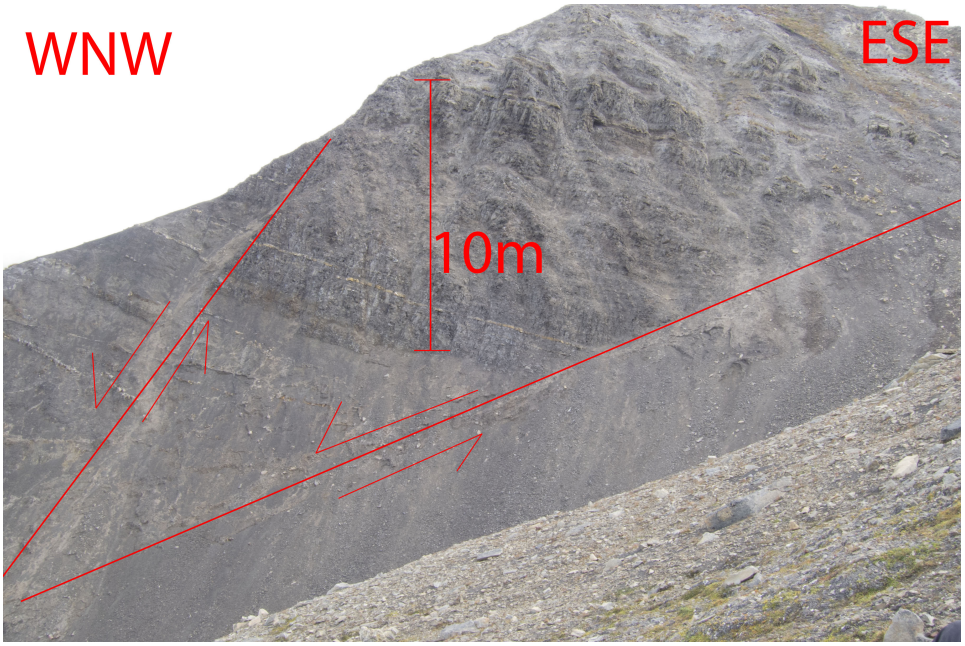

Figure 4.16: Normal faulting within the Rurikfjellet Formation in a fault block.

Figure 4.17: Slope-parallel and slope-normal fracturing in the Kikutodden Member of the Rurikfjellet Formation.

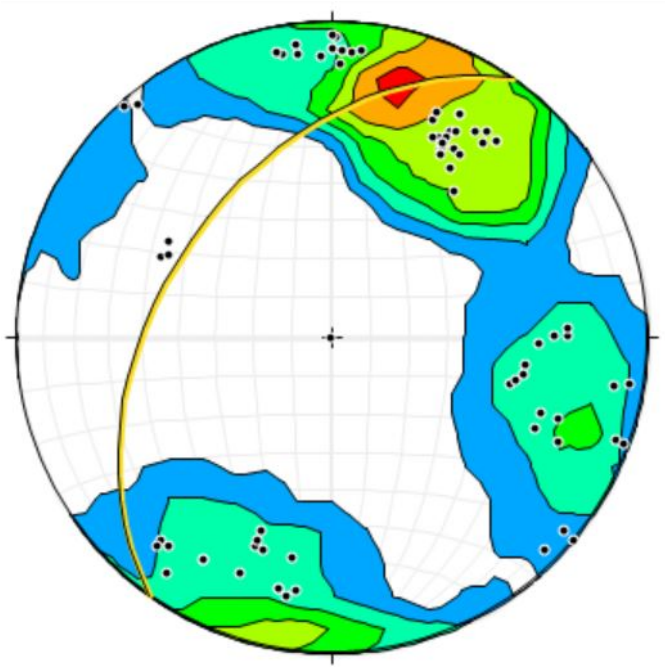

Figure 4.18: Contoured stereoplot (poles) of fracturing in upper Rurikfjellet Formation (Kikutodden Member) with average slope plotted as a plane. Schmidt projection, lower hemisphere with Kamb contouring, 2 sigma intervals.

Figure 4.19: Toppling in a fault block outcrop of the Festningen Member.

4.5.2 Helvetiafjellet Formation

The Festningen Member appears to deform primarily along subvertical fracturing, leading to toppling once underlying shales are removed (Fig. 4.19). Where the Festningen Member is still supported by the underlying Rurikfjellet Formation no apparent fracturing has been found. The heterogenous parts of Helvetiafjellet Formation appear to follow the same trend as the Festningen Member, with coal seams supporting the sandstone packages.

Only 2 intact blocks of the upper parts of the Helvetiafjellet Formation were found in fault blocks. Both of these contain 2 distinct sets of fracture planes (Fig. 4.21), oriented orthogonally to eachother (Fig. 4.20.) Infrequent hydrothermal quartz formation with slickenlineations were observed in these outcrops, but this part of the stratigraphy was not accessible in situ.

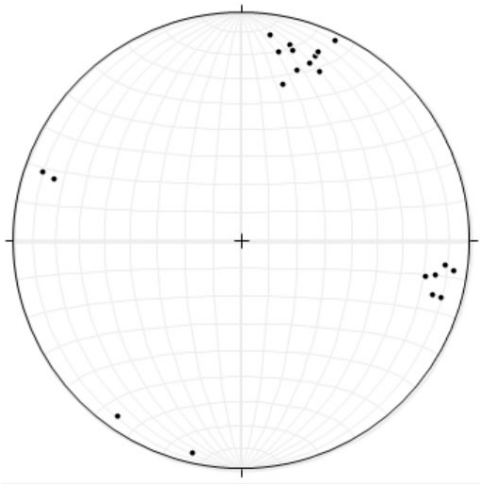

Figure 4.20: Stereoplot of fractures in fault block outcrops of upper Helvetiafjellet Formation. Schmidt projection, lower hemisphere

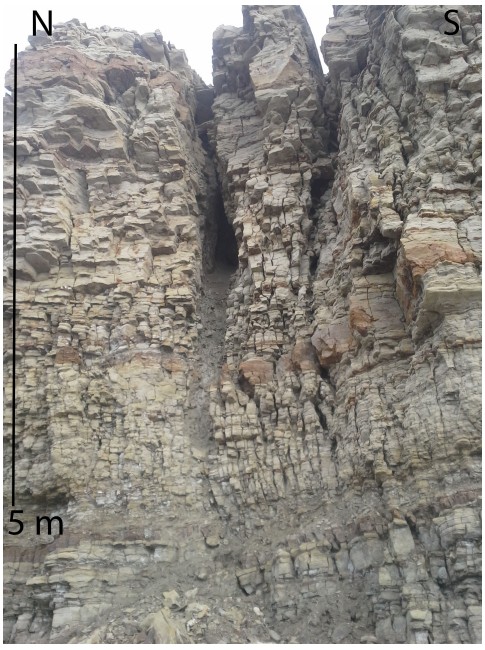

Figure 4.21: Fracturing in a fault block outcrop of upper Helvetiafjellet Formation. The picture shows one set of fracturing, orthogonal to the bedding surfaces.

Chapter 5

Discussion

5.1 Cenozoic deformation structures

The most common type of brittle deformation structures found within the study area is NNW-striking, ENE-dipping reverse faults. The orientation of these faults indicate ENE-WSW-trending σ_1, a NNW-ESE-trending σ_2 and a vertical σ_3. In the context of the WSFTB, these reverse faults are thus hinterland-directed thrusts, or back-thrusts (Fig. 5.2). The general stress field implied by their orientation (Fig. 5.9) fits with the stress field during the transpressional phase of the orogeny (Braathen et al, 1999). Most of the top-to-the-WSW reverse faults have limited displacement, except for the Revneset Reverse Fault which has at least 45 m of vertical displacement (Fig. 4.5). The RRF is antithetical to the Grumantbyen Thrust located on the other side of Adventdalen (Fig. 5.8). On a regional scale, the RRF appears to be one of the few larger back-thrusts cutting Cretaceous strata (Fig. 5.2). It is unclear how deep down into the stratigraphy it cuts before it flattens out, but the closest decollement, in Jurassic strata, makes a plausible candidate for the lower flat (Fig. 5.2).

It is interesting to observe that almost all of the reverse faults further to the east have top-to-the-east displacement (Haremo et al. 1993), whereas the reverse faults within the study area have top-to-the-WSW displacement. A possible explanation for this phenomenom could be the presence of the

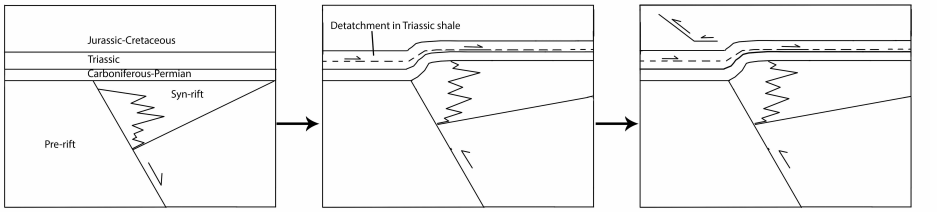

Figure 5.1: Theoretical sketch of the proposed mechanism for back-thrust as a consequence of basin inversion of the Billefjorden Trough. (1) Billefjorden Trough pre-Tertiary deformation. (2) Tertiary shortening and basin inversion folds the less competent post-rift sedimentation, creating space problems in overlying, more competent Jurassic-Cretaceous strata. (3) Back-thrusting along the decollement in the Janusfjellet Subgroup

west-verging monocline associated with basin inversion of the Billefjorden Trough half graben (Haremo et al. 1993). If this monocline was formed prior to or partly prior to eastward propagation of a bedding-parallel thrust in the Agardhfjellet Formation, space problems related to the basin inversion could lead to the formation of back-thrusts such as the RRF (Fig. 5.1).

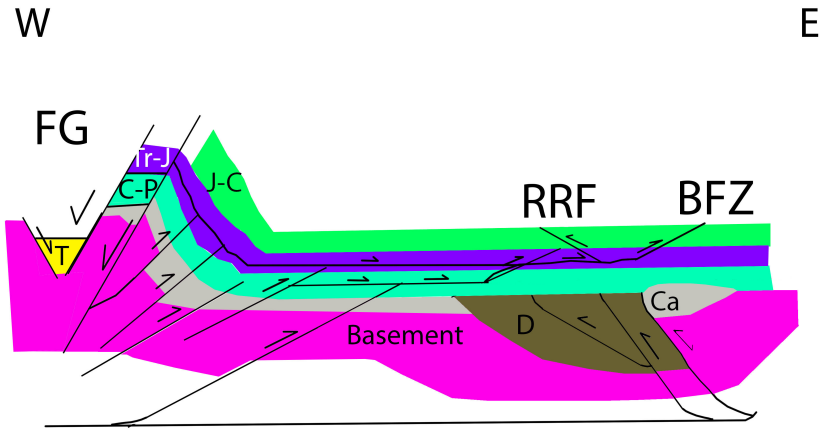

Figure 5.2: Regional scale cross section of important WSFTB-related tectonic elements. FG=Forlandssundet Graben, BFZ=Billefjorden Fault Zone. D=Devonian, Ca=Carboniferous, C-P=Carboniferous-Permian, Tr-J=Triassic-Jurassic, J-C=Jurassic-Cretaceous, T=Tertiary(Cenozoic). Modified from Blinova et al. 2013)

The steep reverse faults observed along the beach north of Revneset (Fig. 4.3, 4.4) appear to terminate structurally downward somewhere in the Rurikfjellet Formation. As the bedding dips towards the NE in this outcrop, the angle between fault plane and bedding are closer to the theoretical 30 degrees common in reverse faulting (Fig. 5.4, 5.5). The difference in dip angle between the steep reverse faults and the RRF suggests that the latter might be an out-of-sequence thrust (Fig. 5.3) If these faults terminate in a roof thrust somewhere in the Rurikfjellet Formation., these structures would be duplexes (Fig. 5.4), while if they terminate without a roof thrust they would form an imbricate fan (Fig. 5.5). Folding of relatively weak layers above the present-day erosional surface could explain the low magnitude of throw along these faults, in which case the steep faults would belong to a blind imbricate fan (Fig. 5.6). As this section of the outcrop is removed by erosion and replaced by glacial till (Fig. 4.3, any roof thrusts or folds that might have existed above the erosional surface are not visible, and as such distinguishing between the different types of splay structures is not possible with the currently available data.

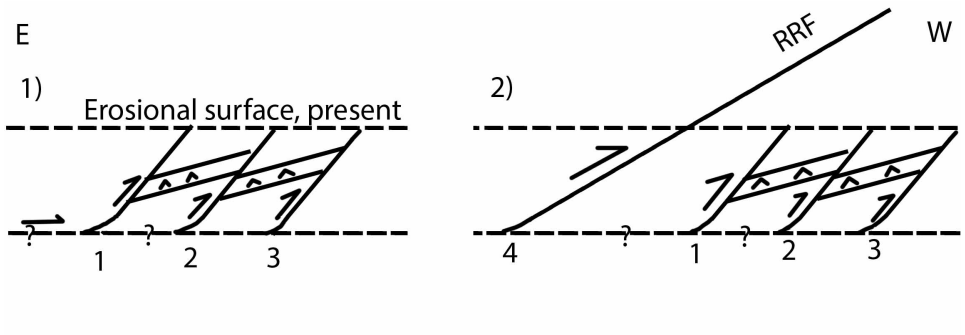

Figure 5.3: Revneset Reverse Fault as an out-of-sequence thrust in relation to the steep reverse faults in the lower Rurikfjellet Formation. outcrop north of Revneset

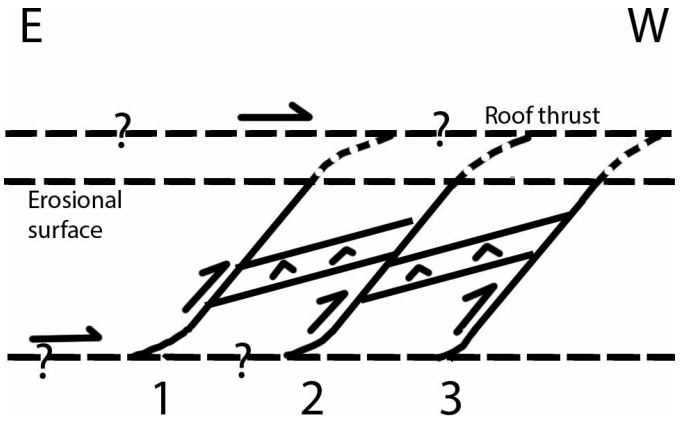

Figure 5.4: Duplex model of the steep reverse faults in the lower Rurikfjellet Formation. outcrop north of Revneset

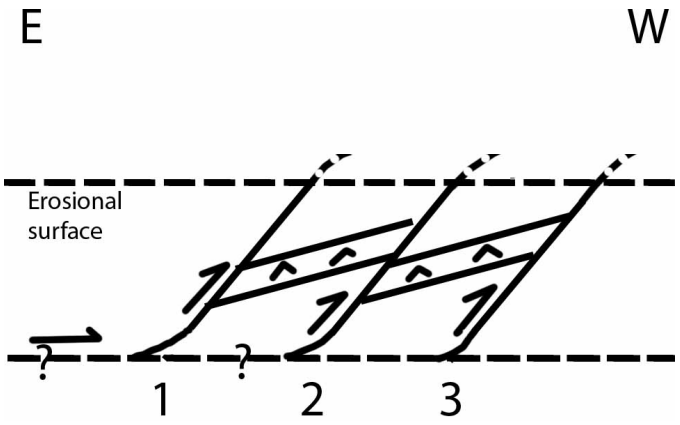

Figure 5.5: Leading imbricate fan model of the steep reverse faults in the lower Rurikfjellet Formation. outcrop north of Revneset

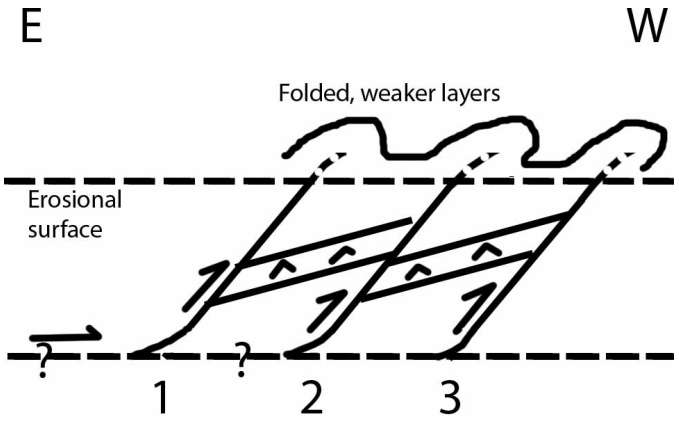

Figure 5.6: Blind imbricate fan model of the steep reverse faults in the lower Rurikfjellet Formation. outcrop north of Revneset. Weak layers above the present-day erosional surface absorbed stress by folding.

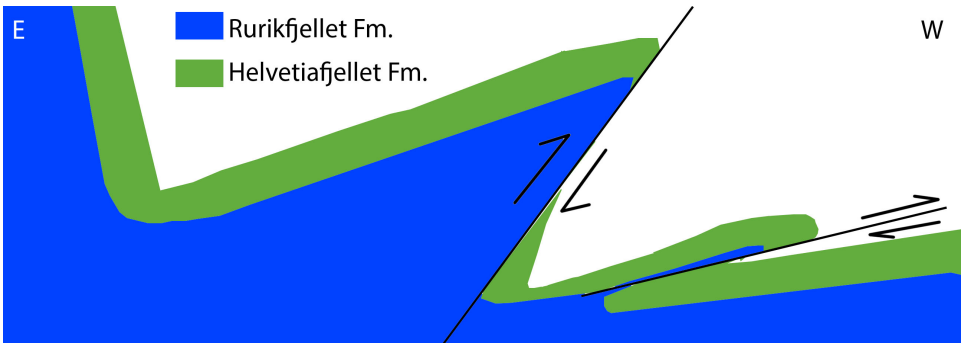

Figure 5.7: Sketch of the Louisdalelva fault-propagation fold system

The Louisdalenelva outcrop displays a steep reverse fault flanked by drag folds on either side. This is interpreted to be a set of fault-propagation folds (Fig. 5.7). Due to its location, and the orientation of its fold axis and fault planes, this structure is interpreted to be a continuation of the Revneset Reverse Fault (Fig. 4.2). Drag folds constitute the only folding visible along the RRF fault plane, this could be due to the outcrop being an oblique view onto the fault plane, or that similar structures as seen in the Louisdalelva outcrop is obscured by scree in the RRF outcrop.

NNW-trending fold axis found in the study area indicate that these structures formed under the same stress regime as the back-thrusts. The orientation of the NE-trending reference fold axis located by Longyearbyen

Airport suggests it originated during the transtensional phase of the WSFTB (Fig. 5.10). Slickenlineations measured at in situ Helvetiafjellet Formation outcrops indicate predominantly normal and left-lateral motion along NW/SE-striking fault planes. The general stress field implied by these movements (Fig. 5.10) fits with the stress field during the transtensional phase of WSFTB formation (Steel 1985).

The boundary normal fault separating the landslide-affected areas from the non-affected areas contains lithified lenses in its fault core, suggesting a pre-glacial age. Both Major's 1964 map and NPI's 2000 map has interpreted this as a boundary fault for a landslide block, suggesting a post-glacial age. This WNW-striking normal fault does not fit the stress regimes of either transtension or transpression suggested by the other structures.

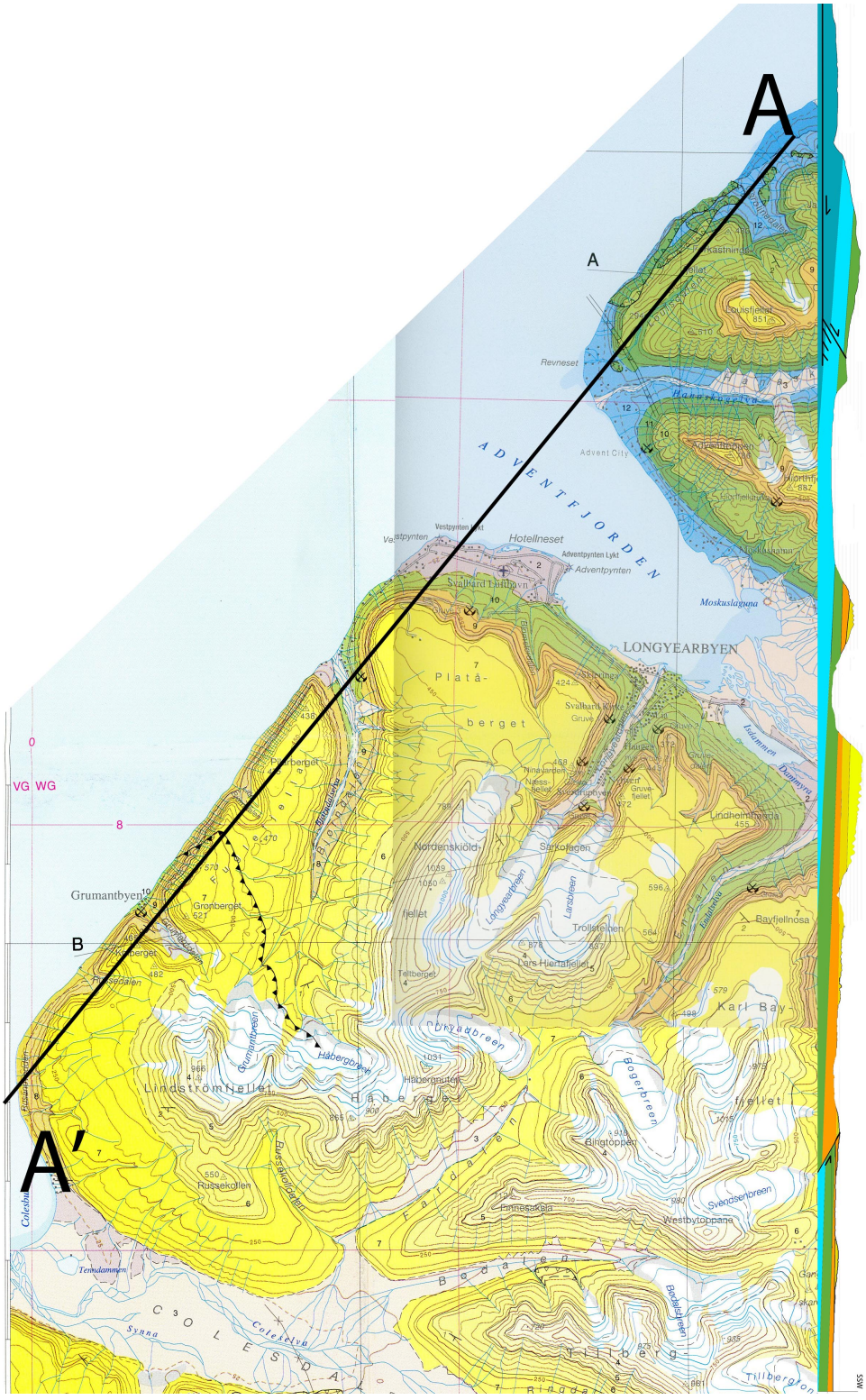

Figure 5.8: Cross-section A-A′ showing the relationship between Revneset Reverse Fault and the Grumantbyen Thrust located on the other side of Adventdalen (2x vertical exaggeration)

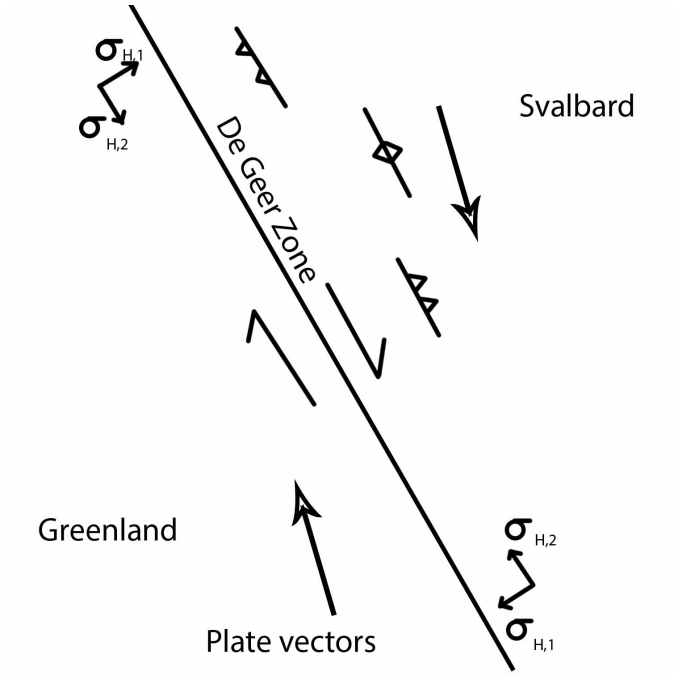

Figure 5.9: Transpressional stress regime during the Eocene. Strain partitioning leads to ENE/WSW shortening. Drawn after Piepjohn et al. 2013

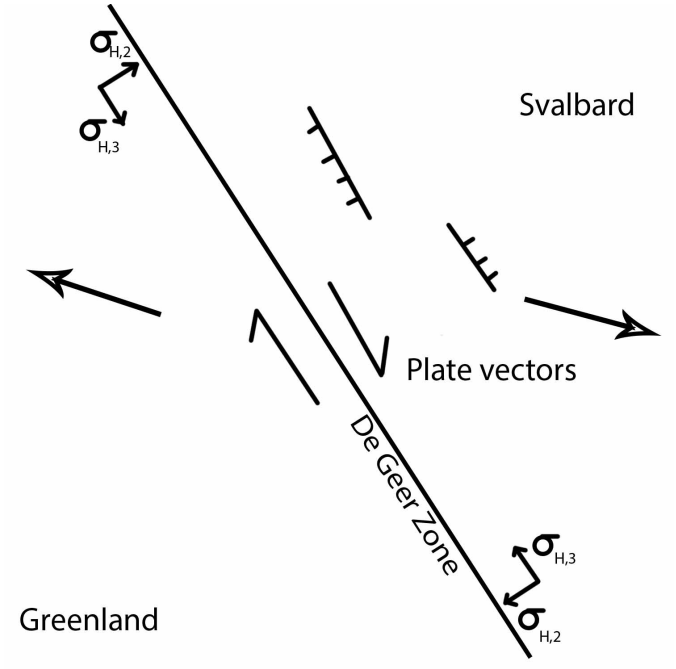

Figure 5.10: Transtensional stress regime during the Oligocene. Strain partitioning leads to NE-SW extension. Drawn after Piepjohn et al. 2013

5.2 Post-glacial deformation structures

5.2.1 Stratigraphic controls on deformation

Internal deformation of fault blocks appear to vary significantly between different lithostratigraphic units. The dark shales of lower Rurikfjellet Formation. deform by high-angle, low-throw normal faulting dipping towards Isfjorden (Fig. 4.16).These faults contain fault cores consisting of fine breccias and gouge.The coarser, silt- to sand-rich Kikutodden Member in the upper Rurikfjellet Formation. contains lenses with highly regular fracture patterns (Fig. 4.17) The massive sandstones of the Festningen Member deform by irregular fracturing (Fig. 4.19), and toppling once underlying units have been removed. Deformation structures involving the Festningen Member suggests that this unit behaves like a rigid block, creating steep topography when it breaks. The alternating shale and sand beds of the upper Helvetiafjellet Formation. display highly regular fracturing (Fig. 4.20, Fig. 4.21).

Fracturing and faulting in both the Festningen Member and the upper part of the Helvetiafjellet Formation. appears to be Mode I fracturing, or jointing. Fracturing in the Kikutodden Member appears to be Mode I for the slope-normal set and Mode II for the slope-parallel set and the slope-oblique set. The different modes of fracture formation suggests that rockfall-type movement is most common in the Helvetiafjellet Formation., and rockslide-type movement is most common in the Rurikfjellet Formation. Differential response to stress between the Festningen Member and both over- and underlying strata in several fault block outcrops (Fig. 4.13,4.14) suggests that the Festningen Member might act as a stratigraphical control on large-scale deformation.

5.2.2 Landslide mechanics

The spatial distribution of distinct fault scarps (Fig. 4.2) suggests several generations of faulting. Three domains of fault scarps have been identified

on the basis of scarp lineaments from DEM and ortophotography (Fig. 5.12). Inferred orientation of fault block rotation axes based on bedding orientation suggests that the fault scarp domain proximal to Isfjorden can be further subdivided into 4 distinct fault blocks. These NE-trending scarps are roughly parallel to the present day Isfjorden coastline. NW-trending fault scarps are believed to represent transfer faults. Variation in the magnitude of secondary rotation suggests that some of these transfer faults are listric in nature, while others appear to induce no secondary rotation and are most likely planar. Secondary block rotation, and a listric transfer fault geometry, has been a criteria for the separation of individual fault blocks (Fig. 5.11). At least 3 additional fault blocks can be inferred from fault scarp distribution, but more bedding orientation data is needed to make a positive identification accordin to the criteria set in this thesis.

Fracture orientation and variation in bedding orientation indicate that rotation of the fault blocks occur on 2 planes, with slope-parallel (scarp-parallel rotation) and slope-normal (counterscarp-parallel rotation). The majority of the rotation is seen along the slope-normal plane, with rotations of upwards of 40 degrees. Both planes exhibit rotation away from the fault plane. Possible explanations for rotation along a fault plane include a listric fault geometry, a scissor fault geometry with rotation along an axis normal to the fault plane, and domino-style stacking of blocks on successive planar faults. The domino-style fault rotation (Wernicke 1981) involves ductile flow of the lower crust to induce rotation, this is unlikely to occur in the case of local, upper crustal brittle tectonics as is believed to be the case here. Scissor faulting is most closely associated with Riedel shear domains under transtensional or transpresional tectonics (Naylor et al. 1986). Two listric fault end-members could explain this rotation; a slumping mechanism with progressive faulting and rotation or a roll-over anticline. Rotational variation within fault blocks suggest slumping being the most prominent mechanism in this area, but roll-over anticlines are present in some fault block outcrops (Fig. 4.13). In the case of slumping, faulting propagates towards the footwall, leading to increased rotation towards the older hanging wall blocks. This mechanism, retrogressive sliding, suggests that

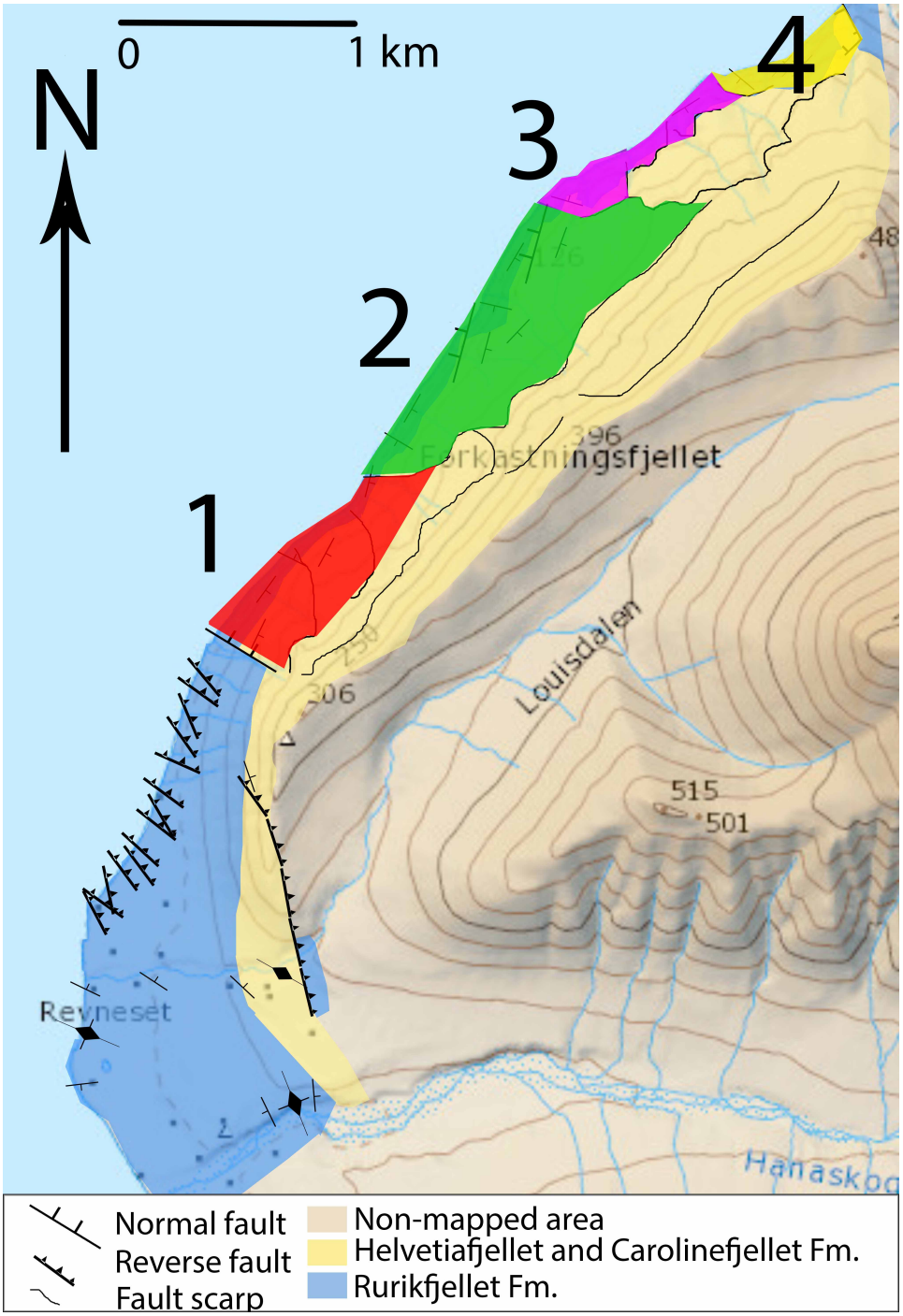

Figure 5.11: Map view with distinct, numbered landslide blocks identified on the basis of secondary block rotation

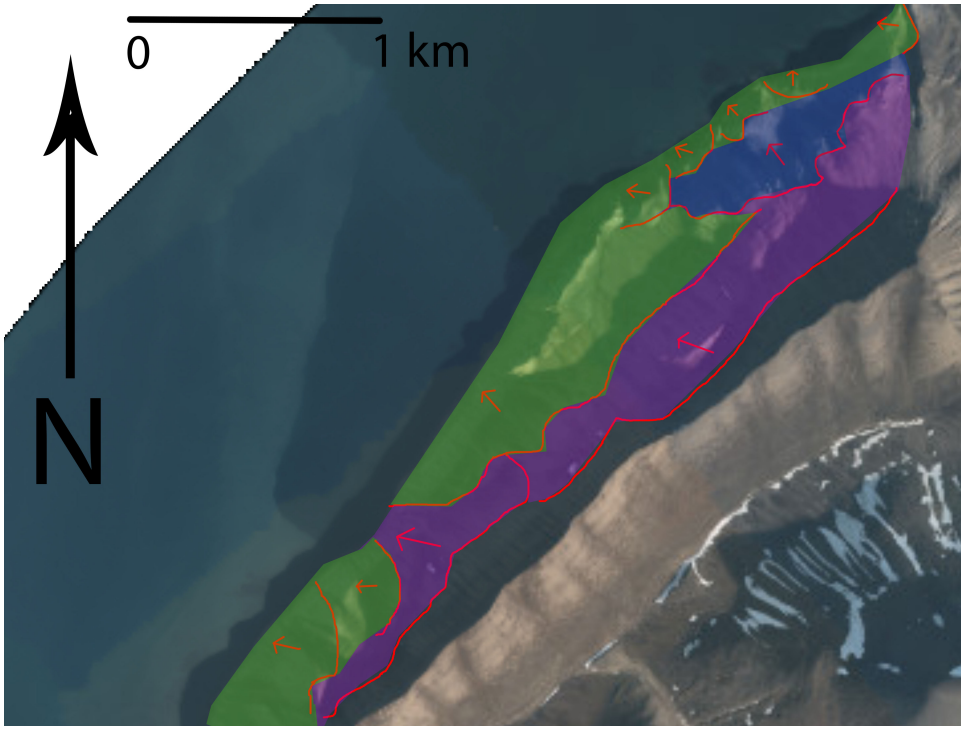

Figure 5.12: Map view of fault scarp domains with proposed movement directions

the fault scarps most distal to Isfjorden are the youngest.

The secondary rotation present in fault blocks could be the result of listric transfer faults orthogonal to the main fault planes.

Although the large-scale faulting appear to follow a listric fault geometry, there are several planar faults present on the tips of several fault blocks (Fig. 4.2) as well as widespread toppling within the Helvetiafjellet Formation. This combination of listric faulting and planar faulting, as well as both rockslide and rockfall deformation conforms to the complex field class of rockslope failure (Braathen et al. 2004).

As the lowest stratigraphical unit exhibiting rotation present in outcrops is the upper part of Rurikfjellet Formation., the detachment has to be lower than this level. In the profile sketch for the proposed landslide mechanics the detachment is placed somewhere in the upper part of the shale-rich Agardfjellet Formation. Bedding planes within this unit is a potential zone of weakness on which a detachment plane might form. The magnitudes of

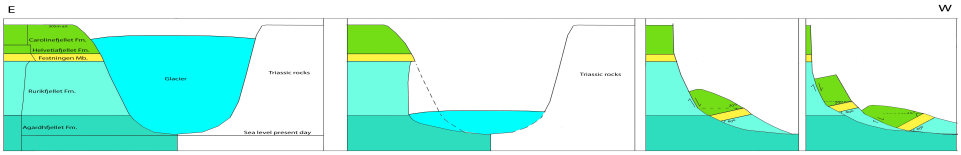

Figure 5.13: Theoretical sketch of the proposed mechanism for landslide formation propagation. Magnitudes of the stratigraphical units are derived from (Braathen et al. 2012)

the stratigraphical units for this sketch are derived from wells drilled on the other side of Adventdalen (Braathen et al. 2012) and the actual magnitudes may differ from those found in the study area. The lower part of Rurikfjellet Formation., the Rurikfjellet Formation.-Agardhfjellet Formation. interface or the upper part of Agardhfjellet Formation. all contain potential zones of weakness, and are as such good candidates for a potential detachment location. Further study of fault geometry and hanging wall deformation is needed to derive a more accurate depth to detachment.

The difference in large-scale (sliding[1]) and small-scale (toppling[2]) deformation mechanics within the Festningen Member indicate two distinct deformation mechanics. In situation [1] the rock undergoes Mode II fracturing and subsequent rotation towards the fault plane (Fig. 5.14). In situation [2] the rock undergoes Mode I fracturing and subsequent rotation away from the fault plane. A possible explanation for this phenomenom is a ramp-flat fault geometry, where the sliding block deforms according to [1] in the part proximal to the fault plane, and according to [2] in the part distal to the fault plane (Fig. 5.14).

If slumping (Fig. 5.13) is the dominant mechanism behind the landslides, domain I (green, Fig. 5.12) is the oldest generation of faulting, followed by domain II (blue) and domain III (red). This sequence of progressive deformation of the footwall is referred to as retrogressive slope failure (Solheim et al. 2005b).

Experimental fracture studies have shown that the Festningen Member is the stratigraphical unit involved in the landslides with the highest tensile

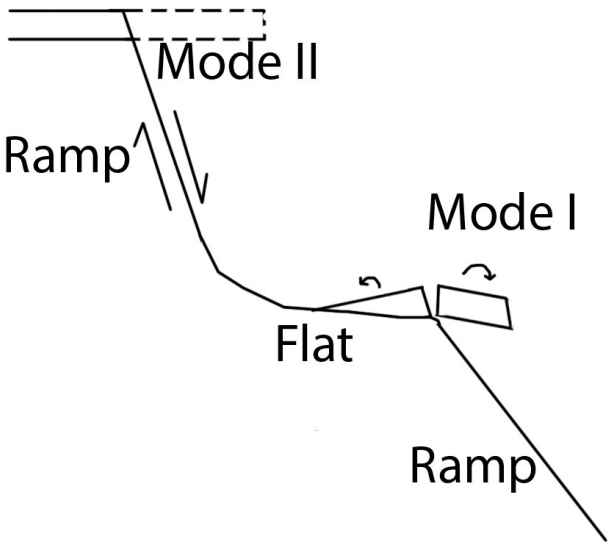

Figure 5.14: Theoretical sketch explaining the different modes of deformation observed in the Festningen Member

strength (Bohloli et al. 2014) and as such would be the determining unit in initiating landslide formation instead of pure glacial erosion. According to the available geological maps (Major 1964; Dallmann et al. 2000), the other side of Isfjorden consists of Triassic rocks, particularly the shale-rich Botnheia Formation. and Vikinghøgda Formation. (Dallmann et al. 1999). As shale-rich rocks would be less resistant to glacial scraping and erosion, and these units are not immediately overlain by units high in tensile strength, a glacial scraping-induced landslide event would not necessarily be symmetrical over Isfjorden.

A possibly analog can be found in the Storegga slide at the Ormen Lange gas field. While the morphology of the area is significantly different, with subhorizontal average slope gradients, the retrogressive, slump-dominated slide mechanisms (Solheim et al. 2005b) are comparable. The geology of the most likely failure plane is also comparable, with marine, water-saturated shales being the dominant lithology of the proposed failure plane(Solheim et al. 2005b; Solheim et al. 2005a).

5.2.3 Origin of extensional stress

The working hypothesis throughout this thesis has been that the landslide-affected areas experienced increased horizontal tensile stress and underwent extensional faulting after glacial retreat at the end of the last ice age. Two possible mechanisms or processes could create such extensional stress after glacial retreat - glacio-eustatic lithospheric rebound as the weight of the icecap is removed (1) and localized scraping of less competent units as the glacier retreats, (2). As the faulting seems to be a localized phenomenom, even along the eastern coast of Isfjorden, (2) appears to be the most likely origin of extensional stress.

Chapter 6

Summary and conclusion

Forkastningsfjellet and its surrounding area contain Cenozoic structures as well as post-glacial landslide structures. The Cenozoic structures are mostly compressional, mainly in the form of top-to-the-west reverse faults, back-thrusts in the context of the WSFTB. The major reverse fault in the area, here called the Revneset Reverse Fault (RRF), is interpreted to be an out-of-sequence thrust relative to the steep reverse faults found in its footwall. While the RRF has a throw of about 45 m, the steeper reverse faults have a throw in the 1-2 m range. Due to glacial erosion a classification of the lesser faults as an imbricate fan or as a duplex is not possible without further studies.

The post-glacial landslides found on the northwestern face of Forkastningsfjellet are interpreted to be a result of glacial erosion of weak layers underlying the rigid Festningen Member sandstone. Fault block rotation indicate a listric fault geometry, with a combination of roll-over anticline formation and slumping being the cause of the bedding rotation. A master detachment is proposed in the Agardhfjellet Formation, with a retrogressive landslide propagation over at least 3 generations of faulting as the likely mechanism. 4 distinct fault blocks have been identified along the coast of Isfjorden, with an additional 3 blocks inferred from fault scarp distribution.

Significant variation in deformation mechanisms between the different

stratigraphical units found in the area is evident from fracture data. The relatively weak Rurikfjellet Formation. fractures easily in several directions, while the Festningen Member sandstone appears to behave as rigid blocks and act as a stratigraphic control on large-scale deformation.

Chapter 7

Suggestions for further work in the area

More detailed field studies need to be carried out to determine the extent of back-thrusts in the area, as well as the presence of other Cenozoic compressional structures, particularly in Louisdalen. Any back-thrusts present without a glacial erosional surface on top would help determining the style of splay formation seen along the coast of Revneset. Traversing along the in situ outcrop of Festningen sandstone could help determine if there are Cenozoic structures present north of the RRF, but safety concerns would require careful planning. Detailed studies of shear deformation in the roll-over anticlines present could assist in determining a depth to the master detachment for the landslides. More detailed studies of internal deformation within fault blocks, especially on the deformation style of the Festningen Member, could shed light on the landslide development and provide parameters for analogue and computaional modelling of the landslide formation. More detailed data on internal deformation could also shed light on the underlying fault geometry. Analogue and computational modelling could determine if glacial scraping is a viable mechanism for providing landslide-inducing stress. Seismic lines along and across Isfjorden could be used to determine the basal decollement for the back-thrusts.

Bibliography

Bælum, K. and A. Braathen (2012). "Along-strike changes in fault array and rift basin geometry of the Carboniferous Billefjorden Trough, Svalbard, Norway." In: *Tectonophysics* 546-547, pp. 38–55.

Bergh, S. G., A. Braathen, and A. Andresen (1997). "Interaction of basement-involved and thin-skinned tectonism in the Tertiary fold-thrust belt of central Spitsbergen, Svalbard." In: *AAPG bulletin* 81.4, pp. 637–661.

Blinova, M. et al. (2013). "Analysis of structural trends of sub-sea-floor strata in the Isfjorden area of the West Spitsbergen Fold-and-Thrust Belt based on multichannel seismic data." In: *Journal of the Geological Society* 170.4, pp. 657–668.

Bohloli, B. et al. (2014). "Evaluation of reservoir and cap-rock integrity for the Longyearbyen CO2 storage pilot based on laboratory experiments and injection tests." In:

Braathen, A., S. G. Bergh, and H. D. Maher (1999). "Application of a critical wedge taper model to the tertiary transpressional fold-thrust belt on Spitsbergen, Svalbard." In: *Bulletin of the Geological Society of America* 111.10, pp. 1468–1485.

Braathen, A. et al. (2004). "Rock-slope failures in Norway; type, geometry, deformation mechanisms and stability." In: *Norsk Geologisk Tidsskrift* 84.1, pp. 67–88.

Braathen, A. et al. (2012). "The Longyearbyen CO." In:

Dallmann, W. K., H Dypvik, and J. G. Gjelberg (1999). *Lithostratigraphic lexicon of Svalbard: Upper Palaeozoic to Quaternary bedrock*. Norsk polarinstitutt Tromso.

Dallmann, W. et al. (2000). *Geological map of Svalbard 1: 100 000, C9G Adventdalen*.

Dypvik, H. (1991). "The Janusfjellet subgroup (Bathonian to Hauterivian) on central Spitsbergen: a revised lithostratigraphy." In: *Polar Research* 9.1, pp. 21–43.

Dypvik, H., E. Håkansson, and C. Heinberg (2002). "Jurassic and Cretaceous palaeogeography and stratigraphic comparisons in the North Greenland-Svalbard region." In: *Polar Research* 21.1, pp. 91–108.

Forwick, M. and T. O. Vorren (2010). "Stratigraphy and deglaciation of the Isfjorden area, Spitsbergen." In: *Norwegian Journal of Geology/Norsk Geologisk Forening* 90.4.

Gasser, D. (2013). "The Caledonides of Greenland, Svalbard and other Arctic areas: status of research and open questions." In: *Geological Society, London, Special Publications* 390.1, pp. 93–129.

Gasser, D. and A. Andresen (2012). "Caledonian terrane amalgamation in Svalbard: Detrital zircon provenance of Mesoproterozoic to Carboniferous strata from Oscar II Land, western Spitsbergen." In: *EGU General Assembly Conference Abstracts* 14, p. 1839.

Gee, D. G. et al. (2008). "From the early Paleozoic platforms of Baltica and Laurentia to the Caledonide orogen of Scandinavia and Greenland." In: *Episodes* 31.March, pp. 44–51.

Gjelberg, J. and R. Steel (2012). "Depositional model for the Lower Cretaceous Helvetiafjellet Formation on Svalbard–diachronous vs. layer-cake models." In: *Norwegian Journal of Geology/Norsk Geologisk Forening* 92.1.

Grosfjeld, K. (1992). "Palynological age constraints on the base of the Helvetiafjellet Formation (Barremian) on Spitsbergen." In: *Polar Research* 11.1, pp. 11–19.

Haremo, P. et al. (1990). "Structural development along the Billefjorden Fault zone in the area between Kjellstromdalen and Advent-

dalen/Sassendalen, central Spitsbergen." In: *Polar Research* 8.2, pp. 195–216.

Haremo, P., A. Andresen, and H. Dypvik (1993). "Mesozoic extension versus Tertiary compression along the Billefjorden Fault Zone south of Isfjorden, central Spitsbergen." In: *Geological Magazine* 130.06, pp. 783–795.

Harland, W. B. and C. B. Wilson (1956). "The Hecla Hoek Succession in Ny Friesland, Spitsbergen." In: *Geological Magazine* 93.04, pp. 265–286.

Ingolfsson, O. (2011). "Fingerprints of Quaternary glaciations on Svalbard." In: *Geological Society, London, Special Publications* 354.1, pp. 15–31.

Maher, H. D. et al. (1995). "Tertiary or Cretaceous age for Spitsbergen's fold-thrust belt on the Barents Shelf." In: *Tectonics* 14.6, pp. 1321–1326.

Maher, H. and A Braathen (2011). "Løvehovden fault and Billefjorden rift basin segmentation and development, Spitsbergen, Norway." In: *Geological Magazine* 148.01, pp. 154–170.

Major, H (1964). "Geological map of Svalbard c9G, Adventdalen, 1: 100 000." In: *Norsk Polarinstitutt*.

Mangerud, J. and J. I. Svendsen (1992). "The last interglacial-glacial period on spitsbergen, Svalbard." In: *Quaternary Science Reviews* 11.6, pp. 633–664.

Midtkandal, I., J. P. Nystuen, and J. Nagy (2007). "Paralic sedimentation on an epicontinental ramp shelf during a full cycle of relative sea-level fluctuation; the Helvetiafjellet Formation in Nordenskiold Land, Spitsbergen." In: *Norwegian Journal of Geology* 87, pp. 343–359.

Midtkandal, I. et al. (2008). "Lower Cretaceous lithostratigraphy across a regional subaerial unconformity in spitsbergen: The Rurikfjellet and Helvetiafjellet Formations." In: *Norsk Geologisk Tidsskrift* 88.4, pp. 287–304.

Naylor, M., G. t. Mandl, and C. Supesteijn (1986). "Fault geometries in basement-induced wrench faulting under different initial stress states." In: *Journal of Structural Geology* 8.7, pp. 737–752.

Nemec, W (1992). “Depositional controls on plant growth and peat accumulation in a braidplain delta environment: Helvetiafjellet Formation (Barremian-Aptian), Svalbard.” In:

Nemec, W. et al. (1988). “Anatomy of collapsed and re-established delta front in Lower Cretaceous of eastern Spitsbergen: gravitational sliding and sedimentation processes.” In: *American Association of Petroleum Geologists Bulletin* 72.4, pp. 454–476.

Piepjohn, K. (2000). “The Svalbardian-Ellesmerian deformation of the Old Red Sandstone and the pre-Devonian basement in NW Spitsbergen (Svalbard).” In: *Geological Society, London, Special Publications* 180.1, pp. 585–601.

Piepjohn, K. et al. (2013). “Ellesmerian and Eurekan fault tectonics at the northern margin of Ellesmere Island (Canadian High Arctic)[Ellesmerische und Eurekan-Störungstektonik am Nordrand von Ellesmere Island (kanadische Hocharktis).]” In: *Zeitschrift der Deutschen Gesellschaft für Geowissenschaften* 164.1, pp. 81–105.

Piepjohn, K. et al. (2015). “Tectonic map of the Ellesmerian and Eurekan deformation belts on Svalbard, North Greenland, and the Queen Elizabeth Islands (Canadian Arctic).” In: *arktos* 1.1, pp. 1–7.

Solheim, A. et al. (1996). “Late Cenozoic depositional history of the western Svalbard continental shelf, controlled by subsidence and climate.” In: *Global and Planetary Change* 12.1-4, pp. 135–148.

Solheim, A. et al. (2005a). “International Centre for Geohazards (ICG): Assessment, prevention and mitigation of geohazards.” In: *Norsk Geologisk Tidsskrift* 85.1-2, pp. 45–62.

Solheim, A. et al. (2005b). “Ormen Lange - An integrated study for the safe development of a deep-water gas field within the Storegga Slide Complex, NE Atlantic continental margin; executive summary.” In: *Marine and Petroleum Geology* 22.1-2 SPEC. ISS. Pp. 1–9.

Steel, R. (1985). “The Tertiary strike-slip basins and orogenic belt of Spitsbergen.” In:

Torsvik, T. H. et al. (2002). "Global reconstructions and North Atlantic paleogeography 440 Ma to recent." In: *BATLAS—Mid Norway plate reconstruction atlas with global and Atlantic perspectives*, pp. 18–39.

Wernicke, B. (1981). "Low-angle normal faults in the Basin and Range Province: nappe tectonics in an extending orogen." In: *Nature* 291, pp. 645–648.

Worsley, D. (1986). *The geological history of Svalbard: evolution of an Arctic archipelago*. Den norske stats oljeselskap as.

— (2008). "The post-Caledonian development of Svalbard and the western Barents Sea." In: *Polar Research* 27.3, pp. 298–317.